


8-2010

## A BAYESIAN APPROACH TO DOSE-RESPONSE ASSESSMENT AND DRUG-DRUG INTERACTION ANALYSIS: APPLICATION TO IN VITRO STUDIES

Violeta G. Hennessey

Follow this and additional works at: [https://digitalcommons.library.tmc.edu/utgsbs\\_dissertations](https://digitalcommons.library.tmc.edu/utgsbs_dissertations)

 Part of the [Biometry Commons](#), [Biostatistics Commons](#), [Other Pharmacy and Pharmaceutical Sciences Commons](#), and the [Statistical Models Commons](#)

---

### Recommended Citation

Hennessey, Violeta G., "A BAYESIAN APPROACH TO DOSE-RESPONSE ASSESSMENT AND DRUG-DRUG INTERACTION ANALYSIS: APPLICATION TO IN VITRO STUDIES" (2010). *The University of Texas MD Anderson Cancer Center UTHealth Graduate School of Biomedical Sciences Dissertations and Theses (Open Access)*. 55.

[https://digitalcommons.library.tmc.edu/utgsbs\\_dissertations/55](https://digitalcommons.library.tmc.edu/utgsbs_dissertations/55)

This Dissertation (PhD) is brought to you for free and open access by the The University of Texas MD Anderson Cancer Center UTHealth Graduate School of Biomedical Sciences at DigitalCommons@TMC. It has been accepted for inclusion in The University of Texas MD Anderson Cancer Center UTHealth Graduate School of Biomedical Sciences Dissertations and Theses (Open Access) by an authorized administrator of DigitalCommons@TMC. For more information, please contact [digitalcommons@library.tmc.edu](mailto:digitalcommons@library.tmc.edu).

A BAYESIAN APPROACH TO DOSE-RESPONSE ASSESSMENT AND  
DRUG-DRUG INTERACTION ANALYSIS: APPLICATION  
TO IN VITRO STUDIES

by

*Violeta G. Hennessey, B.S., M.S.*

APPROVED:

---

Gary L. Rosner, Sc.D., Supervisory Professor

---

J. Jack Lee, D.D.S., Ph.D.

---

Veerabhadran Baladandayuthapani, Ph.D.

---

Yuan Ji, Ph.D.

---

Varsha Gandhi, Ph.D

APPROVED:

---

Dean, The University of Texas  
Graduate School of Biomedical Sciences at Houston

A BAYESIAN APPROACH TO DOSE-RESPONSE ASSESSMENT AND  
DRUG-DRUG INTERACTION ANALYSIS: APPLICATION  
TO IN VITRO STUDIES

A DISSERTATION

Presented to the Faculty of  
The University of Texas  
Health Science Center at Houston  
and  
The University of Texas  
M. D. Anderson Cancer Center  
Graduate School of Biomedical Sciences  
in Partial Fulfillment of the Requirements  
for the Degree of

DOCTOR OF PHILOSOPHY

by

Violeta G. Hennessey, B.S., M.S.  
Houston, Texas

August, 2010

## **Dedication**

To my late father, Michael Conrad Hennessey, and my late grandmother, Rose Hennessey, I wish you were here to share with me the joy of becoming Dr. Hennessey.

## **Acknowledgements**

I would like to express my sincerest gratitude and appreciation to my advisor, Dr. Gary L. Rosner. His mentorship has been crucial in my research development. His intellectual insights and his effort to explain things clearly and simply have brought direction to my research. His reputation and expertise in the field have made him a God-given source of knowledge and wisdom. With all my heart, thank you so very much Gary.

I am particularly thankful to Veerabhadran Baladandayuthapani for his guidance and immense knowledge in semi-parametric methods. I thank you for your patience, motivation, and friendship. I wish to express my warm and sincere thanks to Yuan Ji. His devotion to students should not go un-noticed. Thank you for encouraging and guiding me to meet higher standards. I would like to acknowledge J. Jack Lee for his extraordinary contribution to research in drug interaction analysis. His quality research and writings are matched by his willingness to play a role in my own development as a researcher. I thank you for this. I am grateful to Varsha Gandhi. Her expertise in experimental therapeutics and her insightful comments has proven to be most valuable in my research. My thanks to oncologist Robert C. Bast Jr and members of his lab for their collaboration on the ovarian cancer cell line study.

Finally, I would like to thank my family. Heartfelt thanks to my sister Lorena. I will never forget the time you took away from your family to read my writings and help me think through my ideas. I would like to express my love and gratitude to my mother for her endless support. I have to give a special mention to my husband Youssef. I would not be where I am today without you. I cannot thank you enough.

A BAYESIAN APPROACH TO DOSE-RESPONSE ASSESSMENT AND  
DRUG-DRUG INTERACTION ANALYSIS: APPLICATION  
TO IN VITRO STUDIES

Publication No. \_\_\_\_\_

Violeta G. Hennessey, B.S., M.S.

Supervisory Professor: Gary L. Rosner, Sc.D.

The considerable search for synergistic agents in cancer research is motivated by the therapeutic benefits achieved by combining anti-cancer agents. Synergistic agents make it possible to reduce dosage while maintaining or enhancing a desired effect. Other favorable outcomes of synergistic agents include reduction in toxicity and minimizing or delaying drug resistance. Dose-response assessment and drug-drug interaction analysis play an important part in the drug discovery process, however analysis are often poorly done. This dissertation is an effort to notably improve dose-response assessment and drug-drug interaction analysis.

The most commonly used method in published analysis is the Median-Effect Principle/Combination Index method (Chou and Talalay, 1984). The Median-Effect Principle/Combination Index method leads to inefficiency by ignoring important sources of variation inherent in dose-response data and discarding data points that do not fit the Median-Effect Principle. Previous work has shown that the conventional method yields a high rate of false positives (Boik, Boik, Newman, 2008; Hennessey, Rosner, Bast, Chen, 2010) and, in some cases, low power to detect synergy. There is a great need for improving the current methodology.

We developed a Bayesian framework for dose-response modeling and drug-drug interaction analysis. First, we developed a hierarchical meta-regression dose-response model that accounts for various sources of variation and uncertainty and allows one to incorporate knowledge from prior studies into the current analysis, thus offering a more efficient and reliable inference. Second, in the case that parametric dose-response models do not fit the data, we developed a practical and flexible nonparametric regression method for meta-analysis of independently repeated dose-response experiments. Third, and lastly, we developed a method, based on Loewe additivity that allows one to quantitatively assess interaction between two agents combined at a fixed dose ratio. The proposed method makes a comprehensive and honest account of uncertainty within drug interaction assessment. Extensive simulation studies show that the novel methodology improves the screening process of effective/synergistic agents and reduces the incidence of type I error.

We consider an ovarian cancer cell line study that investigates the combined effect of DNA methylation inhibitors and histone deacetylation inhibitors in human ovarian cancer cell lines. The hypothesis is that the combination of DNA methylation inhibitors and histone deacetylation inhibitors will enhance antiproliferative activity in human ovarian cancer cell lines compared to treatment with each inhibitor alone. By applying the proposed Bayesian methodology, *in vitro* synergy was declared for DNA methylation inhibitor, 5-AZA-2'-deoxycytidine combined with one histone deacetylation inhibitor, suberoylanilide hydroxamic acid or trichostatin A in the cell lines HEY and SKOV3. This suggests potential new epigenetic therapies in cell growth inhibition of ovarian cancer cells.

## Table of Contents

	Page
Dedication.....	iii
Acknowledgments.....	iv
Abstract.....	v
List of Tables.....	x
List of Figures.....	xi
Chapter 1: Introduction .....	1
1.1 Combination Studies... ..	3
1.2 Dose-Response Assessment.....	4
1.3 Drug-Drug Interaction Analysis.....	6
1.4 Motivating Example – Combining DNA Methylation Inhibitors and Histone Deacetylation Inhibitors in Ovarian Cancer Cell Lines.....	8
Chapter 2: Median-Effect Principle / Combination Index Method.....	12
2.1 Overview.....	12
2.2 Standard Meta-Anlaysis.....	12
2.2.1 Dose-Response Assessment .....	12
2.2.2 Drug-Drug Interaction Analysis.....	15
2.3 Analysis of DNA Methylation Inhibitors and Histone Deacetylation Inhibitors In Human Ovarian Cancer Cell Lines.....	18
2.3.1 Study Background.....	18
2.3.2 Results.....	19



## Chapter 3: A Bayesian Approach to Dose-Response Assessment and

Drug-Drug Interaction Analysis.....	27
3.1 Overview.....	27
3.2 Introduction.....	28
3.3 Bayesian Hierarchical Nonlinear $E_{max}$ Model /	
Bayesian Effect Interaction Index Method.....	29
3.3.1 The Model.....	29
3.3.2 Bayesian Posterior Inference.....	32
3.3.2.1 Dose-Response Assessment.....	33
3.3.2.2 Drug-Drug Interaction Analysis.....	33
3.4 Simulation Study.....	35
3.5 Application to the Ovarian Cancer Cell Lines Study.....	43
3.5.1 Dose-Response Assessment.....	46
3.5.2 Assessment of Synergy.....	47

## Chapter 4: Nonparametric Regression Method for Dose-Response Assessment and

Drug-Drug Interaction Analysis.....	54
4.1 Overview.....	54
4.2 Introduction to Monotone Regression I-splines .....	54
4.3 Bayesian Hierarchical Monotone Regression I-splines /	
Bayesian Effect Interaction Index Method.....	56
4.3.1 The Model.....	56
4.3.2 Bayesian Posterior Inference.....	60
4.3.2.1 Dose-Response Assessment.....	60
4.3.2.2 Drug-Drug Interaction Analysis.....	60

4.4 Simulation Study.....	62
Chapter 5: Concluding Remarks.....	69
Appendix A.....	73
Appendix B.....	76
Bibliography.....	78
Vita.....	82

## List of Tables

Table 1.1	List of agents and cell lines under investigation.....	9
Table 2.1	Experiment-specific estimates of the parameters from the linear Median-Effect Principle model and inhibitory concentrations for agents alone and combined in the ovarian cancer cell line HEY.....	21
Table 2.2	Experiment-specific estimates of the parameters from the linear Median-Effect Principle model and inhibitory concentrations for agents alone and combined in the ovarian cancer cell line SKOV-3.....	22
Table 2.3	Meta-analysis results for concentrations that inhibit 25%, 50%, and 75% of the ovarian cancer cell line HEY.....	23
Table 2.4	Meta-analysis results for concentrations that inhibit 25%, 50%, and 75% of the ovarian cancer cell line SKOV-3.....	24
Table 3.1	Parameter values used for generating simulation data.....	36
Table 3.2	Estimates of inhibitory concentrations for DAC alone, SAHA alone, and DAC+SAHA ( $\rho = 0.055$ ) in cell line HEY.....	49

## List of Figures

Figure 1.1	Epigenetic Mechanisms.....	10
Figure 2.1	Combination index versus inhibitory levels for agents in cell line HEY.....	25
Figure 2.2	Combination index versus inhibitory levels for agents in cell line SKOV-3....	26
Figure 3.1	Simulation results for hypothetical agent A.....	38
Figure 3.2	Simulation results for hypothetical agent B.....	39
Figure 3.3	Simulation results for hypothetical agent A + agent B.....	40
Figure 3.4	Simulation results for drug interaction scenario 1, agent B combined with itself (sham experiment).....	42
Figure 3.5	Simulation results for drug interaction scenario 2, agent A combined with agent B produces strong synergy.....	44
Figure 3.6	Simulation results for drug interaction scenario 3, agent A combined with agent B produces qualitatively changing interaction.....	45
Figure 3.7	Fitted dose-response curves for DAC and SAHA, alone and combined, in cell line HEY.....	48
Figure 3.8	Population level dose response curves for combined agents and their respective single-agents in the cell line HEY.....	50
Figure 3.9	Population level dose response curves for combined agents and their respective single-agents in the cell line SKOV3.....	51
Figure 3.10	Boxplots of the posterior distributions of Loewe Interaction	

	Index versus inhibitory level in cell line HEY.....	52
Figure 3.11	Boxplots of the posterior distributions of Loewe Interaction	
	Index versus inhibitory level in cell line SKOV3.....	53
Figure 4.1	I-spline family of degree $r = 2$ associated with	
	$T = 8$ interior knots.....	57
Figure 4.2	Simulation results for Scenario 1 hypothetical agent A.....	64
Figure 4.3	Simulation results for Scenario 1 hypothetical agent B.....	65
Figure 4.4	Simulation results for Scenario 2 hypothetical agent C.....	67
Figure 4.5	Simulation results for Scenario 2 hypothetical agent D.....	68

## Chapter 1: Introduction

In the last 25 years, 1984-2010, thousands of articles have been published in biomedical literature suggesting promise of a single agent or a combination of agents for treating a disease. Dose response assessment and drug-drug interaction analysis play an integral part in the drug discovery process; however, analyses in the literature are often poorly done. An effort is made to improve statistical techniques. Focus is on meta-analysis of independently repeated *in vitro* dose-response experiments. This work is limited to combination studies that combine two agents at a fixed dose ratio.

The conventional method for dose-response assessment and drug interaction analysis is the Median-Effect Principle / Combination Index method (MEPCI). MEPCI uses data preprocessing techniques and transforms a naturally nonlinear dose-response curve into a linear form. The data preprocessing technique often leads to inefficiency by inducing unwanted correlation and deletion of data points that do not follow the theory of MEPCI. The conventional method ignores important sources of variation inherent in the data and uncertainty in parameter values. Previous works have shown the MEPCI can yield high type I error rates (Boik, Boik, Newman, 2008; Hennessey, Rosner, Bast, Chen, 2010) and in some drug-drug interaction cases MEPCI can yield low power to detect synergy (Hennessey, Rosner, Bast, Chen, 2010). The drug development field can benefit from a statistical technique that minimizes errors and maximizes correct decision making, that is, a statistical techniques that ensures future resources are not allocated to false positives and that promising combination agents are not overlooked.

The main objectives of this dissertation are to (1) develop sound predications of dose-response relationship, (2) improve estimator accuracy and precision for inhibitory

concentrations, and (3) improve the screening process of effective/synergistic agents. Novel Bayesian parametric and nonparametric methods have been developed for meta-analysis of independently repeated dose-response experiments. In addition, a novel Bayesian method has been developed to quantitatively assess interaction between two agents combined at a fixed dose ratio.

The remainder of this chapter provides a comprehensive overview of *in vitro* dose-response studies, dose-response assessment, and drug-drug interaction analysis. The motivating ovarian cancer cell line study is also presented. Chapter 2 presents standard meta-analysis with the Median-Effect Principle / Combination Index Method. Step-by-step procedures are shown for preparing the data (data preprocessing) for application of the Median-Effect Principle / Combination Index Method. Analysis of the ovarian cancer cell line study is presented at the end of Chapter 2.

Chapter 3 introduces the proposed Bayesian hierarchical nonlinear  $E_{max}$  model / Bayesian Effect Interaction Index method (BHNE/BEII). This method uses a parametric nonlinear structural model ( $E_{max}$  model) to characterize the relationship between inhibitory response and an agent's concentration level. The Bayesian hierarchical model accounts for variation in the controls, variation within-experiment, variation between-experiments, and heteroscedasticity. Heteroscedasticity is considered because often there is an apparent relationship between mean inhibitory response and variance. The Bayesian Effect Interaction Index method was developed for quantitatively assessing drug-drug interaction with honest accounting of uncertainty. The method bases decision making on the population level posterior distribution of Loewe Interaction Index. A simulation study is reported that evaluates and compares the performance of the BHNE/BEII to meta-analysis with MEPCI. Application of the BHNE/BEII to the ovarian cancer cell line study is presented at the end of Chapter 3.

In the case that dose-response curves exhibit plateaus or other deviations from parametric models, a nonparametric (semi-parametric) regression method was developed under a Bayesian hierarchical framework. Bayesian hierarchical monotone regression I-splines / Bayesian Effect Interaction Index method (BHMI/BEII) is introduced in Chapter 4. The proposed method provides an alternative to parametric regression methods. A simulation study is presented that investigates the performance of the proposed BHMI/BEII in estimating population level dose-response curves and assessing drug-drug interaction. Performance is compared to the parametric methods BHNE/BEII and MEPCI. The ovarian cancer cell line study is analyzed using the nonparametric regression method BHNE/BEII.

Chapter 5 gives concluding remarks and future directions.

## **1.1 Combination Studies**

For many diseases, combination therapies are the norm. Therapies are combined in order to target multiple disease pathways or a single pathway that require multiple agents with different mechanisms. An aim for drug developers is to develop a combination that is synergistic in nature. Synergistic agents provide a way of reducing dosage while maintaining or enhancing efficacy. Synergistic agents can also provide a therapeutic approach to overcome drug resistance.

Candidate agents thought to be effective in treating a disease are first studied *in vitro* as single agents and subsequently in combination. The process for declaring *in vitro* synergy begins with evaluating the dose-response of each agent alone and combined. Results are compared via an additive model to determine the presence of synergy.

A typical *in vitro* dose-response study will include independently repeated experiments. In each experiment, a multi-well tray is utilized with an equal number of cells plated to each



well. Wells are then grouped (replicates) and assigned control wells (no drug) or receive one of the investigating concentration levels. Typically, a small number (less than ten) of concentration levels are investigated. After days of treatment, viability of the cells is evaluated using an assay. Investigators will typically repeat independent experiments to ensure reproducibility. The same experimental design is used for combination studies, with the exception that agents may be combined using a fixed dose ratio.

## 1.2 Dose-Response Assessment

Dose-response assessment involves fitting dose-response curves and estimating inhibitory concentrations (concentration required to inhibit some fraction of cells). In this dissertation, dose and concentration are used interchangeably. Regression analysis is used to model the relationship between response and an agent's concentration level. A general dose-response regression model is

$$y_i = f(c_i, \boldsymbol{\theta}) + \boldsymbol{\varepsilon}_i,$$

and includes the following:

- the dependent response variable,  $Y$
- the independent variable drug concentration,  $C$
- the structural model relating  $Y$  and  $C$ ,  $f(C, \boldsymbol{\theta})$
- the vector of unknown parameters denoted as  $\boldsymbol{\theta}$
- the random error term,  $\boldsymbol{\varepsilon}$ , reflecting omitted factors that influence response

For a continuous response, common parametric structural models used are the Median-Effect equation (Chou and Talalay, 1984),

$$\frac{f_a}{f_u} = \left( \frac{C}{IC_{50}} \right)^M \quad (1.1)$$

and the Emax model (Hill, 1910; Greco, 1995; Lee et al., 2007),

$$Y = \frac{E_0}{1 + \left( \frac{C}{IC_{50}} \right)^M} \quad (1.2)$$

The Median-Effect equation (1.1) models the response variable, fraction of cells affected  $f_a$  with  $f_u = 1 - f_a$ . The  $E_{max}$  model (1.2) differs in that it models measured response  $Y$  and allows one to model the variation in the controls through the parameter  $E_0$ ; the Median-Effect model (1.1) does not allow this. The  $E_0$  in the  $E_{max}$  model (1.2) represents  $E(Y)$  when  $C = 0$ . In both models,  $C$  is the drug concentration;  $IC_{50}$  is the concentration producing 50% inhibition; and  $M$  is a Hill-type coefficient (shape parameter).

The Median-Effect method requires the observed data to be normalized by the control response (response in the absence of drug) and forces a naturally nonlinear dose-response relationship into a linear form through variable transformations.

$$\log(f_a/f_u) = -M * \log(IC_{50}) + M * \log(C) = \beta_0 + \beta_1 * \log(C) \quad (1.3)$$

A linear regression analysis is typically less accurate than a nonlinear regression analysis (Boik et al., 2008; Hennessey et al., 2010) but is commonly used because of its simplicity.

An alternative to parametric regression methods are nonparametric (semi-parametric) regression methods. Semi-parametric regression splines use piece-wise basis functions to approximate the mean response function  $f(C)$ . The type of basis function employed (e.g., truncated polynomials, low-rank thin plate splines, natural cubic splines, B-splines, M-splines, I-splines) may be motivated by concern about numerical stability, ease of implementation, interpretability, or curve characteristics (Ruppert, Wand, and Carroll, 2003). In the context of *in vitro* dose-response curves, characteristics may be smooth and monotone.

### 1.3 Drug-Drug Interaction Analysis

Drug-drug interaction can occur when two or more single-agents are combined. Types of interactions are additive, synergistic, and antagonistic. Synergistic interaction is when the combined effect is greater than additive. Antagonistic interaction is when the combined effect is less than additive. When performing interaction analysis, it is important to clearly define effect and additive.

Current methodologies make use of additive (reference) models, algebraic formulations to characterize additivity. Two rival additive models are Bliss independence (Bliss, 1939) and Loewe additivity (Loewe and Muischnek, 1926). The Bliss independence is based on the idea of probabilistic independence, that is, the combined effect (e.g., fractional response) is equal to the product of the effect of each agent alone. Greco (1995) explains Bliss independence as two agents acting in such a manner that neither one interferes with the other, but each contributes to a common result. Loewe additivity is based on the idea of a sham experiment; that is, an agent combined with itself cannot interact with itself (Greco, 1995). Comparison of the two reference models has been the subject of many articles (Goldoni and Johansson, 2007; Greco et al, 1995; Lee et al., 2007). This dissertation considers the Loewe additivity model, since it has received a greater amount of support in the literature and is the basis of many interaction assessment approaches (Greco et al., 1995; Lee et al., 2007). Goldoni and Johansson (2007) also argue that the Loewe additivity model has slightly higher biological plausibility.

The Loewe additivity model for two agents can be expressed as

$$1 = \frac{d_A}{D_A} + \frac{d_B}{D_B}. \quad (1.4)$$

In the numerators,  $d_A$  and  $d_B$  represent the doses of agent A and agent B, respectively, in combination, that result in a specific effect (e.g., 50% inhibition). In the denominators,  $D_A$  and  $D_B$  are the doses of agent A alone and agent B alone, respectively, resulting in the same specific

effect. The sum on the right hand side of the equation is referred to as the Loewe interaction index. In the case of additivity, the Loewe interaction index equals one. A Loewe interaction index less (greater) than one corresponds to synergy (antagonism) (Greco et al, 1995).

Chou and Talalay (1984) proposed plots of the interaction index versus fraction of cells affected ( $f_a$ ) for drugs combined at a fixed dose-ratio (single-ray design). This method is referred to as the Combination Index method and has been addressed as the most commonly used method for quantifying synergy. Chou and Talalay (1984) imply that the combination index (CI) is equal to Loewe interaction index when the drugs obey the Median-Effect principle and the effects of the drugs are mutually exclusive (i.e., they have the same modes of action).

$$CI = \frac{d_A}{D_A} + \frac{d_B}{D_B} \quad (1.5)$$

If the drugs are mutually nonexclusive (i.e., they have different modes of actions), Chou and Talalay (1984) suggest an additional term in the sum.

$$CI = \frac{d_A}{D_A} + \frac{d_B}{D_B} + \frac{d_A d_B}{D_A D_B} \quad (1.6)$$

In practice, however, the additional term is rarely used and confidence intervals for the interaction index are constructed to perform hypothesis testing of additivity. Lee and Kong (2007) point out that the confidence intervals in published analysis are constructed using a normal assumption. Lee and Kong (2007) explain that this assumption may not be appropriate, considering that the interaction index takes only positive values ( $CI > 0$ ). Lee and Kong (2007) suggest that a normal assumption on the log scale is more appropriate. The 95% confidence interval for CI is then constructed by

$$\exp[\log(CI) \pm t_{df,0.975} \sqrt{\text{Var}(\log(CI))}]. \quad (1.7)$$

where  $t_{df,0.975}$  is the 97.5<sup>th</sup> percentile of  $t$ -distribution with degree of freedom  $df$ . The degree of freedom is equal to the number of data points used to compute CI minus the total number of

estimated parameters involved in estimating CI. Lee and Kong (2006) use the delta method to approximate the variance of  $\log(CI)$ . It is then suggested that one concludes additivity when the 95% confidence interval includes the value one. Synergy is concluded when  $CI < 1$  and all values in the 95% confidence interval fall below one. Antagonism is concluded when  $CI > 1$  and all values in the 95% confidence interval lie above one.

#### **1.4 Motivating Example – Combining DNA Methylation Inhibitors and Histone Deacetylation Inhibitors in Ovarian Cancer Cell Lines**

Oncologists in the Department of Experimental Therapeutics at The University of Texas MD Anderson Cancer Center were interested in investigating the combined effect of DNA methylation inhibitors and histone deacetylation inhibitors in human ovarian cancer cell lines. The list of agents and cell lines under investigation is provided in Table 1.1.

DNA methylation inhibitors and histone deacetylation inhibitors are considered epigenetic therapies. Epigenetic mechanisms such as DNA methylation and histone deacetylation control gene expression without changing the DNA sequence. Methylation of DNA is a chemical method to silence a gene. Histone deacetylation is a structural method that condenses chromatin structure preventing transcription, replication, and repair (Figure 1.2). Both mechanisms are important for normal cellular development, but can be overly active in carcinogenesis. It is believed that inhibition of DNA methylation and histone deacetylation will result in re-expression of tumor suppressor genes and reverse oncogenesis. DNA methylation inhibitors and histone deacetylation inhibitors have been investigated as single agent therapies. They are known to induce death in cancer cells but not in normal cells. Little is known about the combined effect in ovarian cancer cell lines. The hypothesis is that the combination of DNA methylation inhibitors and histone deacetylation inhibitors will enhance anti-

**Table 1.1 List of agents and cell lines under investigation.** The first column lists two human ovarian cancer cell lines. The second column lists the epigenetic targets. The third column describes the class of agents. The fourth column lists the agents under investigation. Agents are investigated as single-agents alone and in combination (the different classes are paired).

Cell Line	Target	Class	Agents
HEY	DNA methylation	DNA methylation inhibitors	5-Aza-2'-deoxycytidine (decitabine)
			5-Azacytidine (azacitidine)
	histone deacetylation	histone deacetylation inhibitors	Suberoylanilide hydroxamic acid (SAHA)
			Trichostatin A (TSA)
SKOV-3	DNA methylation	DNA methylation inhibitors	5-Aza-2'-deoxycytidine (decitabine)
			5-Azacytidine (azacitidine)
	histone deacetylation	histone deacetylation inhibitors	Suberoylanilide hydroxamic acid (SAHA)
			Trichostatin A (TSA)

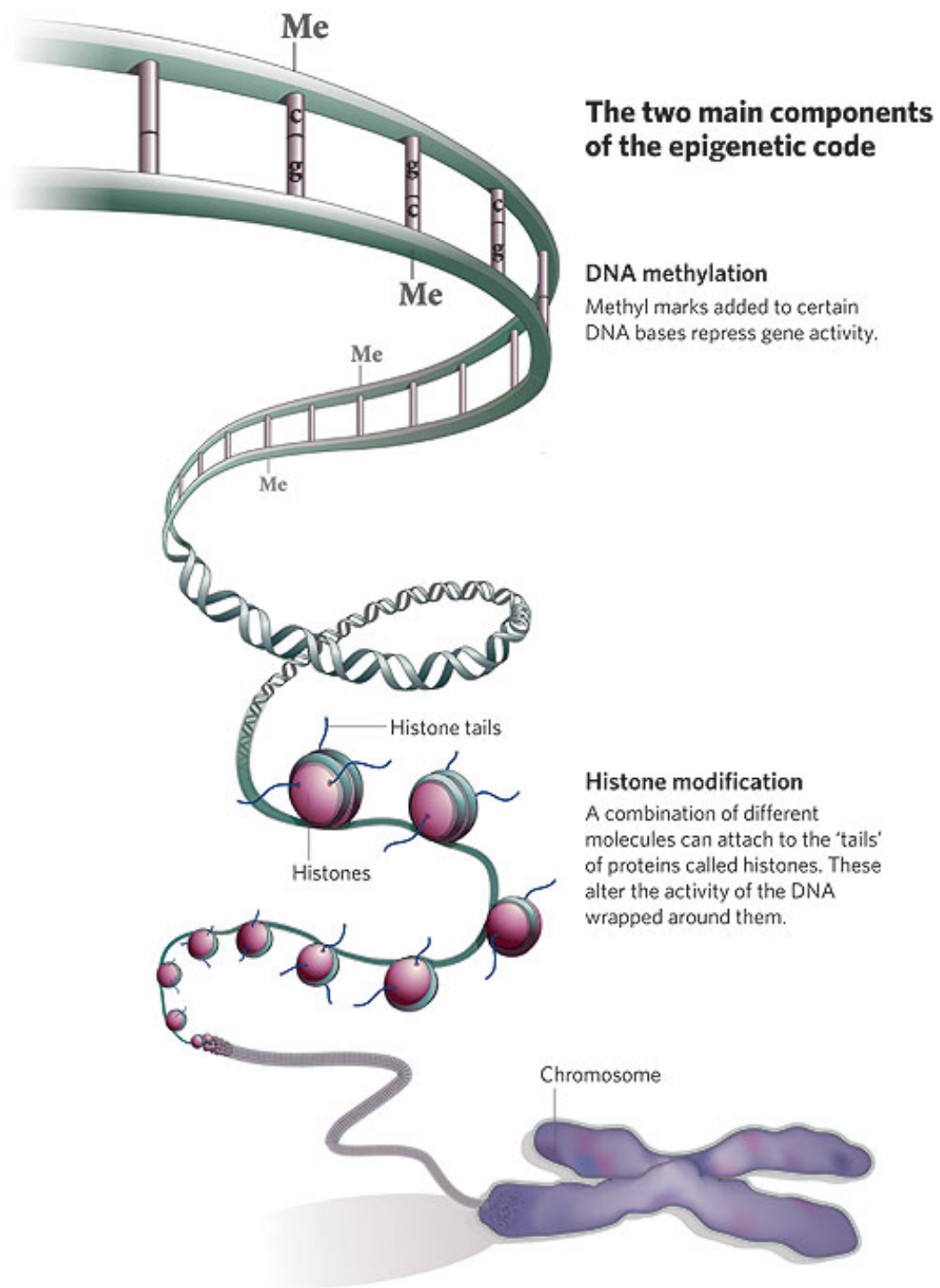


**Figure 1.1: Epigenetic Mechanisms.** DNA methylation is a chemical method to silence genes. Histone deacetylation increases the affinity of the histones to bind to the DNA, preventing transcription. Reprinted by permission from Macmillan Publishers Ltd: Nature 441, 143-145, copyright (11 May 2006).

proliferative activity in ovarian cancer cell lines compared to the single agents.



## **Chapter 2: Median-Effect Principle / Combination Index Method**

### **2.1 Overview**

The Median-Effect Principle / Combination Index method (Chou and Talalay, 1984) is the most commonly used method for dose-response assessment and quantitative analysis of drug-drug interaction. The Median-Effect Principle / Combination Index method is derived under the mass-action law principle and provides a theoretical basis for (i) relating response and an agent's concentration level and (ii) assessing interaction between two or more combined agents. Chou (2006) claims the popularity of the Median-Effect Principle / Combination Index method can be attributed to its simplicity and its ability to relate to other major biochemical and biophysical equations. Such equations include the Michaelis-Menten equation, Henderson-Hasselbalch equation, Scatchard equation, and the Hill's equation.

The purpose of this chapter is to provide details of the Median-Effect Principle / Combination Index methods and step-by-step procedures for data preprocessing and meta-analysis of independently repeated experiments. Real data analyses are illustrated with the ovarian cancer cell line study.

### **2.2 Standard Meta-Analysis with the Median-Effect Principle / Combination Index Method**

#### **2.2.1 Dose-Response Assessment**

The Median-Effect method addresses dose-response assessment for a single-agent and has been extended to two or more combined agents (Chou, 1991). The Median-Effect equation considers the following dose-response relationship

$$F_a = \frac{1}{1 + \left(\frac{C}{IC_{50}}\right)^M} \quad (2.1)$$

where  $F_a$  is the dependent response variable, fraction affected. The independent variable is  $C$ , the agent's concentration. The parameters to be estimated are  $IC_{50}$  (concentration producing 50% inhibition), and  $M$  known as the Hill's coefficient. Chou (1976, 1977) simplifies the nonlinear dose-response relationship into a linear form by regressing  $\log f_a$  on  $\log c$ .

$$\log \left( \frac{f_{a,i}}{1 - f_{a,i}} \right) = \beta_0 + \beta_1 \log(c_i) + \varepsilon_i \quad (2.2)$$

The coefficients  $\beta_0$  and  $\beta_1$  relate to the parameters  $IC_{50}$  and  $M$  through  $\beta_0 = M * \log(IC_{50})$  and  $\beta_1 = M$ . Interest in estimating inhibitory concentrations ( $IC_x$  = the concentration producing  $x\%$  inhibition) requires an inverse function of the coefficients from the fitted model.

$$\widehat{IC}_x = \exp \left( -\frac{\hat{\beta}_0}{\hat{\beta}_1} \right) \left( \frac{x}{100 - x} \right)^{\frac{1}{\hat{\beta}_1}} \quad (2.3)$$

For studies with independently repeated experiments, standard meta-analysis procedures perform separate analysis to each experiment and take a weighted average of the separate estimates. Below we provide step-by-step procedures for standard meta-analysis. Also given are standard data preprocessing steps, variable transformation, and model fitting techniques for Median-Effect analysis.

#### Data Preprocessing:

1. For each concentration level, replicates are averaged within-experiment.
2. For each experiment, divide the average responses by the average control response.

This results in fraction unaffected ( $f_u$ ).

3. To obtain  $f_a$ , subtract  $f_u$  from 1 ( $f_a = 1 - f_u$ ).
4. Data points that fall outside the allowed (0, 1) range are deleted.

Variable Transformation:

1. Take the logit transformation of the dependent variable , that is,  $\log[f_a/(1-f_a)]$  .
2. Take the log transformation of the independent variable, that is,  $\log (C)$ .

Model Fitting:

1. logit  $f_a$  is regressed on  $\log c$ . A separate linear model (2.2) is fit to each experimental data using ordinary least squares technique (OLS). OLS uses a numerical search procedure to find the values of  $\beta_0$  and  $\beta_1$  that minimize the least squares criterion  $Q$ .

$$Q = \sum_{i=1}^n \left( \log \left( \frac{f_{a,i}}{1-f_{a,i}} \right) - \beta_0 - \beta_1 \log(c_i) \right)^2$$

2.  $R^2$  is used as a measure of goodness of fit (or how well the data obeys the mass-action principle). An  $R^2 < 0.81$  is considered a poor fit and the experimental data are not considered in the meta-analysis.

$$R^2 = \frac{\sum_{i=1}^n \left( \hat{\beta}_0 + \hat{\beta}_1 \log(c_i) - \overline{\log \left( \frac{f_{a,i}}{1-f_{a,i}} \right)} \right)^2}{\sum_{i=1}^n \left( \log \left( \frac{f_{a,i}}{1-f_{a,i}} \right) - \overline{\log \left( \frac{f_{a,i}}{1-f_{a,i}} \right)} \right)^2}$$

The meta-analysis takes a weighted average of the separate estimates. The variance (standard errors squared) are used as weights. For example, a weighted average  $\overline{IC}_x^{(w)}$  is estimated by

$$\overline{IC}_x^{(w)} = \frac{\sum_{e=1}^E \frac{1}{se^2(\widehat{IC}_x^{(e)})} * \widehat{IC}_x^{(e)}}{\sum_{e=1}^E \frac{1}{se^2(\widehat{IC}_x^{(e)})}} \quad (2.4)$$

where  $e$  indexes experiment and  $E$  is the number of repeated experiments included in the meta-analysis. The variance of each  $\widehat{IC}_x^{(e)}$  can be approximated using the delta method (Bickel and Doksum, 2001; Lee and Kong, 2007).

$$\begin{aligned}
 se^2(\widehat{IC}_x^{(e)}) &= \text{var}(\widehat{IC}_x^{(e)}) \\
 &\approx \widehat{IC}_x^{2(e)} \\
 &\quad * \left( \frac{\text{var}(\hat{\beta}_0^{(e)})}{\hat{\beta}_1^{2(e)}} + \frac{2 * \text{cov}(\hat{\beta}_0^{(e)}, \hat{\beta}_1^{(e)}) * \left(\log\left(\frac{100-x}{x}\right) - \hat{\beta}_0^{(e)}\right)}{\hat{\beta}_1^{3(e)}} \right. \\
 &\quad \left. + \frac{\text{var}(\hat{\beta}_1^{(e)}) * \left(\log\left(\frac{100-x}{x}\right) - \hat{\beta}_0^{(e)}\right)^2}{\hat{\beta}_1^{4(e)}} \right) \quad (2.5)
 \end{aligned}$$

Interval estimates of  $\overline{IC}_x^{(w)}$  can be given by constructing the 95% confidence interval

$$\exp \left[ \log(\overline{IC}_x^{(w)}) \pm t_{df, 0.975} \sqrt{\text{var}(\log(\overline{IC}_x^{(w)}))} \right], \quad (2.6)$$

where, by the delta method

$$\begin{aligned}
 \text{var}(\log(\overline{IC}_x^{(w)})) &\cong \frac{1}{\overline{IC}_x^{(w)2}} * \text{var}(\overline{IC}_x^{(w)}) \\
 &\cong \frac{1}{\overline{IC}_x^{(w)2}} * \frac{1}{\left( \frac{1}{se^2(\widehat{IC}_x^{(1)})} + \frac{1}{se^2(\widehat{IC}_x^{(2)})} + \dots + \frac{1}{se^2(\widehat{IC}_x^{(E)})} \right)} \quad (2.7)
 \end{aligned}$$

### 2.2.2 Drug-Drug Interaction Analysis

The Combination Index method quantitatively assesses interaction between two agents combined at a fixed dose-ratio (single-ray design) and can be extended to three or more agents.

The combination index ( $CI$ ) for  $x$  % inhibition is estimated by

$$\widehat{CI}_x = \frac{\widehat{IC}_{x,A+B} * \left(\frac{\omega}{1+\omega}\right)}{\widehat{IC}_{x,A}} + \frac{\widehat{IC}_{x,A+B} * \left(\frac{1}{1+\omega}\right)}{\widehat{IC}_{x,B}}. \quad (2.8)$$

In the numerators,  $\widehat{IC}_{x,A+B}$  is a point estimate of  $IC_x$  for the combined agents (agent A + agent B) and  $\omega$  is the fixed-dose ratio ( $\omega = c_A/c_B$ ). In the denominators,  $\widehat{IC}_{x,A}$  and  $\widehat{IC}_{x,B}$  are point estimates of  $IC_x$  for agent A alone and agent B alone, respectively. The estimates of the input parameters are computed using equation (2.3) with  $\hat{\beta}_0$  and  $\hat{\beta}_1$  taken from agent-specific fitted dose-response curves as described in Section 2.2.1.

For meta-analysis, one computes an estimate of  $CI_x$  for each experiment. The weighted average  $\overline{CI}_x^{(w)}$  is estimated by

$$\overline{CI}_x^{(w)} = \frac{\sum_{e=1}^E \frac{1}{se^2(\widehat{CI}_x^{(e)})} * \widehat{CI}_x^{(e)}}{\sum_{e=1}^E \frac{1}{se^2(\widehat{CI}_x^{(e)})}}, \quad (2.9)$$

where again  $e$  indexes experiment, and  $E$  is the number of repeated experiments included in the meta-analysis. The variance of each  $\widehat{CI}_x^{(e)}$  can be approximated using the delta method (Bickel and Doksum, 2001; Lee and Kong, 2007).

$$\begin{aligned}
\text{se}^2(\widehat{CI}_x^{(e)}) &\cong \text{var}(\widehat{CI}_x^{(e)}) \\
&\cong \left( \frac{\widehat{IC}_{x,A+B}^{(e)} * \left( \frac{\omega}{1+\omega} \right)}{\widehat{IC}_{x,A}^{(e)}} \right)^2 \\
&* \left( \frac{\text{var}(\hat{\beta}_{0,A}^{(e)})}{\hat{\beta}_{1,A}^{2(e)}} + \frac{2 * \text{cov}(\hat{\beta}_{0,A}^{(e)}, \hat{\beta}_{1,A}^{(e)}) * \left( \log\left(\frac{100-x}{x}\right) - \hat{\beta}_{0,A}^{(e)} \right)}{\hat{\beta}_{1,A}^{3(e)}} \right. \\
&+ \frac{\text{var}(\hat{\beta}_{1,A}^{(e)}) * \left( \log\left(\frac{100-x}{x}\right) - \hat{\beta}_{0,A}^{(e)} \right)^2}{\hat{\beta}_{1,A}^{4(e)}} \left. + \left( \frac{\widehat{IC}_{x,A+B}^{(e)} * \left( \frac{1}{1+\omega} \right)}{\widehat{IC}_{x,B}^{(e)}} \right)^2 \right. \\
&* \left( \frac{\text{var}(\hat{\beta}_{0,B}^{(e)})}{\hat{\beta}_{1,B}^{2(e)}} + \frac{2 * \text{cov}(\hat{\beta}_{0,B}^{(e)}, \hat{\beta}_{1,B}^{(e)}) * \left( \log\left(\frac{100-x}{x}\right) - \hat{\beta}_{0,B}^{(e)} \right)}{\hat{\beta}_{1,B}^{3(e)}} \right. \\
&+ \frac{\text{var}(\hat{\beta}_{1,B}^{(e)}) * \left( \log\left(\frac{100-x}{x}\right) - \hat{\beta}_{0,B}^{(e)} \right)^2}{\hat{\beta}_{1,B}^{4(e)}} \left. + \left( \widehat{CI}_x^{(e)} \right)^2 \right. \\
&* \left( \frac{\text{var}(\hat{\beta}_{0,A+B}^{(e)})}{\hat{\beta}_{1,A+B}^{2(e)}} \right. \\
&+ \frac{2 * \text{cov}(\hat{\beta}_{0,A+B}^{(e)}, \hat{\beta}_{1,A+B}^{(e)}) * \left( \log\left(\frac{100-x}{x}\right) - \hat{\beta}_{0,A+B}^{(e)} \right)}{\hat{\beta}_{1,A}^{3(e)}} \\
&+ \frac{\text{var}(\hat{\beta}_{1,A+B}^{(e)}) * \left( \log\left(\frac{100-x}{x}\right) - \hat{\beta}_{0,A+B}^{(e)} \right)^2}{\hat{\beta}_{1,A+B}^{4(e)}} \left. \right) \quad (2.10)
\end{aligned}$$

Hypothesis testing of additivity is performed at the 0.05 level of significance by constructing the 95% confidence interval for  $\widehat{CI}_x^{(w)}$ .

$$\left[ \overline{CI}_x^{(w)} * \exp\left(\frac{-t_{df,0.975}}{\overline{CI}_x^{(w)}} * \sqrt{var(\overline{CI}_x^{(w)})}\right), \overline{CI}_x^{(w)} * \exp\left(\frac{t_{df,0.975}}{\overline{CI}_x^{(w)}} * \sqrt{var(\overline{CI}_x^{(w)})}\right) \right] \quad (2.11)$$

where

$$var(\overline{CI}_x^{(w)}) \cong \frac{1}{\left( \frac{1}{se^2(\overline{CI}_x^{(1)})} + \frac{1}{se^2(\overline{CI}_x^{(2)})} + \dots + \frac{1}{se^2(\overline{CI}_x^{(E)})} \right)} \quad (2.12)$$

It is suggested that one concludes additivity when the 95% confidence interval includes the value one. Synergy is concluded when  $\overline{CI}_x^{(w)} < 1$  and all values in the 95% confidence interval fall below one. Antagonism is concluded when  $\overline{CI}_x^{(w)} > 1$  and all values in the 95% confidence interval lie above one.

## 2.3 Analysis of DNA Methylation Inhibitors and Histone Deacetylation Inhibitors In

### Human Ovarian Cancer Cell Lines

We apply the Median-Effect Principle/Combination Index method to real data from an ovarian cancer cell line study. Investigators were interested in assessing effective doses of each agent (see Table 1.1) that inhibit 25%, 50%, and 75% of the ovarian cancer cell lines. They were also interested in evaluating combinations of DNA methylation inhibitors and histone deacetylation inhibitors that might enhance antiproliferative activities (i.e., synergistic interaction).

#### 2.3.1 Study Background

In brief, human ovarian cancer cells, HEY and SKOV3, were treated with single agent treatments of DNA methylation inhibitors and histone deacetylation inhibitors or their combinations (different classes of inhibitors are combined). The DNA methylation inhibitors

are AZA(0-100 $\mu$ M) and DAC(0-100 $\mu$ M) with concentration ranges shown in parenthesis. The histone deacetylation inhibitors are TSA(0-2 $\mu$ M), and SAHA(0-32 $\mu$ M).

For each agent and cell line combination, ten concentration levels were investigated (serial 2-fold changes) including control ( $C = 0$ ). After five days of treatment, sulforhodamine B (SRB) assay (Skehan et al., 1990) was carried out and the number of cells surviving was expressed in optical density measurements (OD). Independent experiments were repeated three times with each experiment containing three replicates per concentration level. For combination studies, DNA methylation inhibitors, AZA and DAC, are combined with histone deacetylation inhibitors, TSA and SAHA. A single ray design is used to combine agents; that is, agents are combined using a fixed dose ratio.

### 2.3.1 Results

Table 2.1 displays experiment-specific estimates of the parameters from the linear Median-Effect Principle for agents alone and combined in the ovarian cancer cell line HEY. Table 2.2 displays experiment-specific estimates for treated SKOV3 cells. The linear model (2.2) was fit to each experimental data using ordinary least squares as implemented in R with the function *lm*. An estimate of the linear model parameters, the standard errors of the parameters, correlation between the parameters and a measure of goodness of fit  $r^2$  is provided. An  $r^2 < 0.81$  is considered a poor fit and results are not considered for meta-analysis. Estimates of inhibitory concentrations and their standard errors are calculated using equation (2.3) and equation (2.7) respectively. Table 2.3 and Table 2.4 displays the meta-analysis weighted  $\overline{IC}_{25}^{(w)}$ ,  $\overline{IC}_{50}^{(w)}$ ,  $\overline{IC}_{75}^{(w)}$  and their standard errors in the cell lines HEY and SKOV3, respectively.

Figure 2.1 and Figure 2.2 displays results from drug-drug interaction analysis for cell lines HEY and SKOV3, respectively. We graphically display results by plotting combination



index versus inhibitory levels. The blue points represent the point estimates of the weighted combination index  $\overline{CI}_x^{(w)}$ . The black dashes represent the 95% upper and lower confidence limit. Synergy is concluded when  $\overline{CI}_x^{(w)} < 1$  and the 95% confidence interval falls below 1. Additivity is concluded if the 95% confidence interval includes the value 1. Antagonism is concluded when  $\overline{CI}_x^{(w)} > 1$  and the 95% confidence interval lies above.

For the cell line HEY, synergy is concluded for DAC+SAHA and DAC+TSA at all inhibitory levels. For the cell line SKOV3, synergy is concluded for DAC+SAHA at all inhibitory levels and DAC+TSA at inhibitory levels 30-85%.

**Table 2.1. Experiment-specific estimates of the parameters from the linear Median-Effect Principle model and inhibitory concentrations for agents alone and combined in the ovarian cancer cell line HEY.** The linear model (2.2) was fit using ordinary least squares as implemented in R with the function *lm*. An estimate of the linear model parameters, the standard errors of the parameters, correlation between the parameters and a measure of goodness of fit  $r^2$  is provided. An  $r^2 < 0.81$  is considered a poor fit and results are not considered. Estimates of inhibitory concentrations and their standard errors are calculated using equation (2.3) and equation (2.7) respectively.

Agent	experiment	$\hat{\beta}_0$	$se(\hat{\beta}_0)$	$\hat{\beta}_1$	$se(\hat{\beta}_1)$	$corr(\hat{\beta}_0, \hat{\beta}_1)$	$r^2$	$\hat{IC}_{25}$	$se(\hat{IC}_{25})$	$\hat{IC}_{50}$	$se(\hat{IC}_{50})$	$\hat{IC}_{75}$	$se(\hat{IC}_{75})$
DAC	1	-2.29	0.13	0.56	0.051	-0.72	0.94	8.30	3.42	58.49	15.15	412.0	67.5
	2	-2.06	0.16	0.54	0.064	-0.72	0.91	6.00	3.16	46.22	14.78	356.0	75.9
	3	-2.09	0.14	0.66	0.056	-0.72	0.95	4.50	1.33	23.68	4.50	124.6	19.3
AZA	1	-2.81	0.54	1.59	0.21	-0.72	0.89	2.94	0.74	5.88	1.39	11.75	3.01
	2	-2.89	0.36	1.62	0.14	-0.72	0.95	3.03	0.50	5.97	0.93	11.78	1.98
	3	-6.12	0.92	2.43	0.32	-0.84	0.92	7.85	1.68	12.32	2.49	19.34	4.01
SAHA	1	-1.78	0.72	1.77	0.31	-0.90	0.91	1.47	0.28	2.72	0.70	5.06	1.75
	2	-1.13	0.15	1.58	0.077	-0.55	0.99	1.02	0.082	2.04	0.16	4.10	0.38
	3	-0.28	0.32	1.43	0.17	-0.55	0.92	0.57	0.11	1.22	0.26	2.63	0.71
TSA	1	4.19	0.92	2.12	0.47	0.71	0.82	0.083	0.025	0.14	0.05	0.23	0.09
	2	4.10	0.95	1.87	0.60	0.66	0.71	-	-	-	-	-	-
	3	4.05	0.59	1.71	0.25	0.74	0.89	0.049	0.011	0.09	0.02	0.18	0.05
DAC+SAHA ( $\omega = 18.22$ )	1	0.069	0.14	0.72	0.043	-0.85	0.98	0.20	0.026	0.91	0.18	4.15	1.18
	2	1.10	0.066	0.45	0.020	-0.85	0.99	0.007	0.001	0.085	0.02	0.99	0.35
	3	0.024	0.15	0.70	0.044	-0.85	0.97	0.20	0.028	0.97	0.21	4.61	1.39
DAC+TSA ( $\omega = 366$ )	1	-0.092	0.24	0.75	0.07	-0.84	0.94	0.26	0.055	1.13	0.36	4.92	2.19
	2	0.66	0.24	0.52	0.07	-0.84	0.88	0.03	0.012	0.28	0.17	2.32	2.10
	3	-0.37	0.30	0.83	0.089	-0.84	0.93	0.41	0.092	1.56	0.50	5.89	2.59
AZA+SAHA ( $\omega = 4.4$ )	1	-2.63	0.46	1.53	0.19	-0.67	0.90	2.73	0.67	5.60	1.24	11.49	2.69
	2	-2.80	0.41	1.50	0.17	-0.67	0.92	3.11	0.72	6.46	1.32	13.43	2.80
	3	-2.71	0.49	1.80	0.20	-0.77	0.94	2.45	0.43	4.51	0.81	8.30	1.71
AZA+TSA ( $\omega = 88$ )	1	-2.23	0.51	1.51	0.23	-0.62	0.87	2.12	0.61	4.38	1.15	9.09	5.55
	2	-3.85	0.40	2.16	0.17	-0.66	0.97	3.58	0.53	5.97	0.83	9.93	1.39
	3	-2.89	0.35	1.86	0.16	-0.62	0.95	2.62	0.42	4.74	0.70	8.56	1.30

**Table 2.2. Experiment-specific estimates of the parameters from the linear Median-Effect Principle model and inhibitory concentrations for agents alone and combined in the ovarian cancer cell line SKOV-3.** The Median-Effect linear model was fitted using ordinary least squares as implemented in R with the function `lm`. An estimate of the linear model parameters, the standard errors of the parameters, correlation between the parameters, and a measure of goodness of fit  $r^2$  is provided. An  $r^2 < 0.81$  is considered a poor fit and results are not considered. Estimates of inhibitory concentrations and their standard errors are also provided and calculated using equation (2.3) and equation (2.7) respectively.

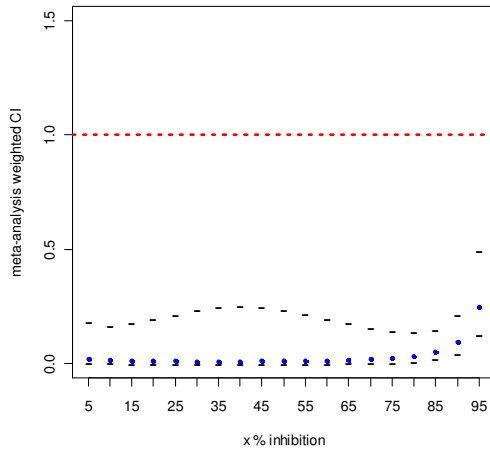
Agent	experiment	$\hat{\beta}_0$	$se(\hat{\beta}_0)$	$\hat{\beta}_1$	$se(\hat{\beta}_1)$	$corr(\hat{\beta}_0, \hat{\beta}_1)$	$r^2$	$\hat{IC}_{25}$	$se(\hat{IC}_{25})$	$\hat{IC}_{50}$	$se(\hat{IC}_{50})$	$\hat{IC}_{75}$	$se(\hat{IC}_{75})$
DAC	1	-2.20	0.31	0.28	0.12	-0.72	0.43	-	-	-	-	-	-
	2	-0.81	0.17	0.17	0.065	-0.72	0.48	-	-	-	-	-	-
	3	-2.45	0.20	0.42	0.075	-0.81	0.84	25.25	29.23	347	247	4782	1624
AZA	1	-2.10	0.52	0.74	0.19	-0.77	0.72	-	-	-	-	-	-
	2	-3.12	0.44	1.33	0.16	-0.81	0.92	4.57	1.04	10.42	2.03	23.76	4.98
	3	-4.20	0.39	1.26	0.11	-0.98	0.99	11.62	0.97	27.69	1.89	65.99	7.55
SAHA	1	-1.78	0.72	1.77	0.31	-0.90	0.91	1.82	0.62	3.17	1.07	5.51	2.11
	2	-1.13	0.15	1.58	0.077	-0.55	0.99	0.62	0.077	1.43	0.17	3.30	0.47
	3	-0.28	0.32	1.43	0.17	-0.55	0.92	0.23	0.03	0.70	0.11	2.11	0.46
TSA	1	3.93	0.84	1.86	0.36	0.74	0.82	0.067	0.021	0.12	0.038	0.22	0.08
	2	3.01	0.31	1.033	0.11	0.76	0.92	0.019	0.004	0.05	0.011	0.16	0.04
	3	3.58	0.53	1.50	0.22	0.74	0.88	0.044	0.010	0.09	0.02	0.19	0.06
DAC+SAHA ( $\omega = 29.81$ )	1	0.78	0.28	0.70	0.08	0.81	0.91	0.61	0.14	3.06	0.91	14.75	6.58
	2	-1.75	0.24	0.80	0.07	-0.84	0.95	2.24	0.39	8.81	1.50	34.64	8.34
	3	-1.12	0.16	0.79	0.04	-0.89	0.98	1.02	0.09	4.12	0.55	16.62	3.33
DAC+TSA ( $\omega = 546$ )	1	-0.92	0.26	0.80	0.08	-0.84	0.94	0.80	0.15	3.17	0.77	12.48	4.36
	2	-1.49	0.33	0.83	0.10	-0.84	0.91	1.61	0.35	6.03	1.47	22.67	7.88
	3	-1.63	0.86	0.49	0.26	-0.84	0.34	-	-	-	-	-	-
AZA+SAHA ( $\omega = 16.7$ )	1	-3.46	0.81	1.50	0.23	-0.94	0.91	4.82	0.89	10.02	2.38	20.82	6.69
	2	-5.43	2.05	1.86	0.54	-0.97	0.81	10.27	2.96	18.55	6.63	33.50	16.11
	3	-3.16	0.33	1.35	0.11	-0.79	0.95	4.60	0.77	10.38	1.57	23.44	3.84
AZA+TSA ( $\omega = 306$ )	1	-3.01	1.13	1.40	0.30	-0.97	0.88	3.91	1.00	8.59	3.25	18.85	9.95
	2	-2.10	1.09	1.23	0.29	-0.97	0.86	2.26	0.75	5.50	2.77	13.41	9.34
	3	-4.78	0.70	1.76	0.24	-0.78	0.88	8.09	2.36	15.09	3.87	28.15	6.98

**Table 2.3. Meta-analysis results for concentrations that inhibit 25%, 50%, and 75% of the ovarian cancer cell line HEY.** Estimates of  $\overline{IC}_{25}^{(w)}$ ,  $\overline{IC}_{50}^{(w)}$ ,  $\overline{IC}_{75}^{(w)}$  and their standard errors are calculated using equation (2.4) and equation (2.7) respectively.

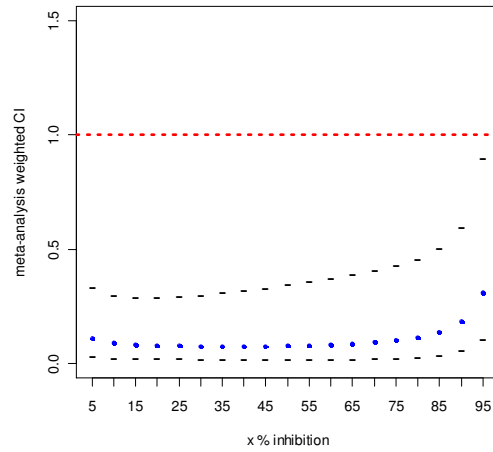
Agent	$\widehat{IC}_{25}^{(w)}$	$se(\widehat{IC}_{25}^{(w)})$	$\widehat{IC}_{50}^{(w)}$	$se(\widehat{IC}_{50}^{(w)})$	$\widehat{IC}_{75}^{(w)}$	$se(\widehat{IC}_{75}^{(w)})$
DAC	5.13	1.34	28.04	17.13	158.17	325.14
AZA	3.28	0.16	6.50	0.55	12.86	2.34
SAHA	0.88	0.004	1.85	0.02	3.82	0.11
TSA	0.055	0.001	0.10	0.0004	0.19	0.002
DAC+SAHA ( $\omega = 18.22$ )	0.0077	1.14E-6	0.10	0.0004	1.45	0.10
DAC+TSA ( $\omega = 366.44$ )	0.05	1.4E-4	0.53	0.022	4.15	1.71
AZA+SAHA ( $\omega = 4.4$ )	2.64	0.10	5.16	0.36	10.10	1.64
AZA+TSA ( $\omega = 88$ )	2.79	0.084	5.09	0.24	9.18	0.79

**Table 2.4. Meta-analysis results for concentrations that inhibit 25%, 50%, and 75% of the ovarian cancer cell line SKOV-3.** Estimates of  $\overline{IC}_{25}^{(w)}$ ,  $\overline{IC}_{50}^{(w)}$ ,  $\overline{IC}_{75}^{(w)}$  and their standard errors are calculated using equation (2.4) and equation (2.7) respectively.

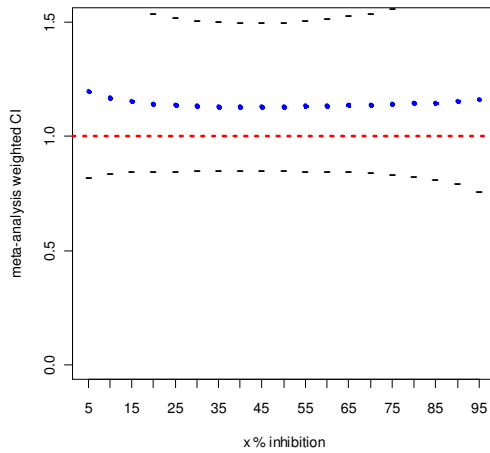
Agent	$\widehat{IC}_{25}^{(w)}$	$se(\widehat{IC}_{25}^{(w)})$	$\widehat{IC}_{50}^{(w)}$	$se(\widehat{IC}_{50}^{(w)})$	$\widehat{IC}_{75}^{(w)}$	$se(\widehat{IC}_{75}^{(w)})$
DAC	25.25	29.23	347	247	4782	1624
AZA	8.32	0.51	19.61	1.91	36.53	17.26
SAHA	0.29	0.0009	0.94	0.0089	2.76	0.11
TSA	0.022	1.13E-5	0.065	9.8E-5	0.18	0.001
DAC+SAHA ( $\omega = 29.81$ )	0.95	0.0058	4.29	0.20	18.32	7.82
DAC+TSA ( $\omega = 546$ )	0.92	0.01	3.78	0.46	14.86	14.53
AZA+SAHA ( $\omega = 16.7$ )	4.91	0.33	10.58	1.65	23.33	10.65
AZA+TSA ( $\omega = 306$ )	3.17	0.34	8.70	3.43	21.90	23.77



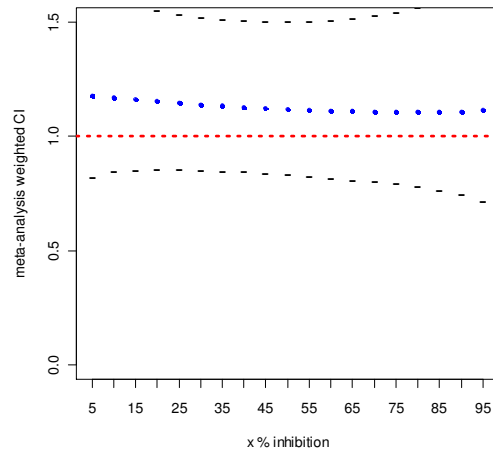
(a) DAC+SAHA



(b) DAC+TSA



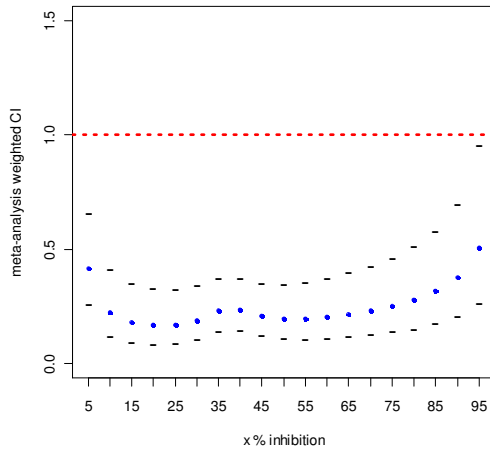
(a) AZA+SAHA



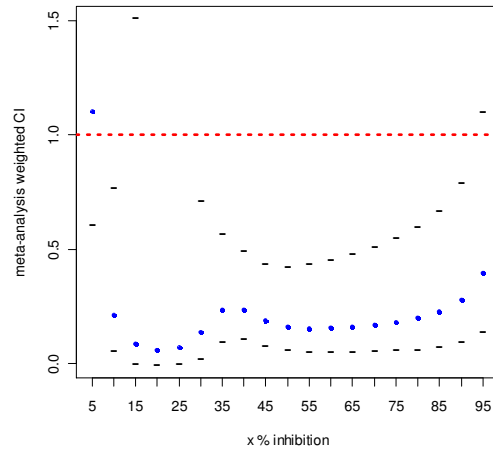
(b) AZA+TSA

**Figure 2.1 Combination index versus inhibitory levels for agents in cell line HEY.**

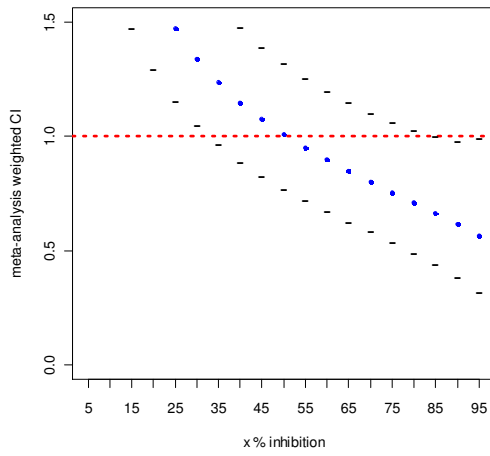
The blue points represent the point estimates of the weighted combination index  $\overline{CI}_x^{(w)}$ . The black dashes represent the 95% upper and lower confidence limit. Synergy is concluded when  $\overline{CI}_x^{(w)} < 1$  and the 95% confidence interval falls below 1. (a) For DAC + SAHA synergy is concluded for all inhibitory levels. (b) For DAC + TSA synergy is concluded for all inhibitory levels. (c) For AZA+SAHA additivity is concluded for inhibitory levels. (d) For AZA+TSA additivity is concluded for all inhibitory levels.



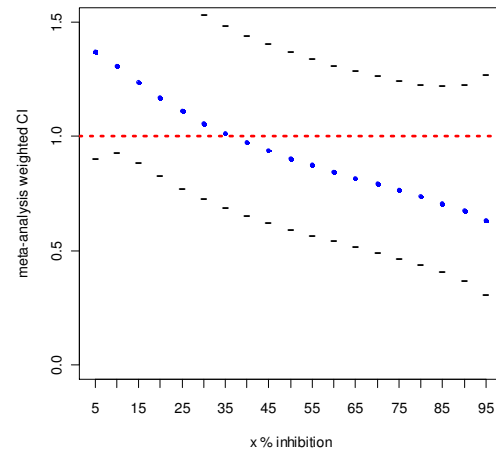
(a) DAC+SAHA



(b) DAC+TSA



(c) AZA+SAHA



(d) AZA+TSA

**Figure 2.2 Combination index versus inhibitory levels for agents in cell line SKOV3.**

The blue points represent the point estimates of the weighted combination index  $\overline{CI}_x^{(w)}$ . The black dashes represent the 95% upper and lower confidence limit. Synergy is concluded when  $\overline{CI}_x^{(w)} < 1$  and the 95% confidence interval falls below 1. (a) For DAC + SAHA synergy is concluded for all inhibitory levels. (b) For DAC + TSA synergy is concluded for inhibitory levels 30-90%. (c) For AZA+SAHA antagonism is concluded for inhibitory levels below 30%, additivity for inhibitory levels above 30%. (d) For AZA+TSA additivity is concluded.

## Chapter 3: A Bayesian Approach to Dose-Response Assessment and Drug-Drug Interaction Analysis

### 3.1 Overview

This chapter provides an alternative Bayesian framework for dose-response assessment and drug-drug interaction analysis. Bayesian statistics differs from classical frequentist statistics. In Bayesian statistics, parameters are treated as random quantities instead of fixed unknown quantities. A probability distribution (prior) is used to describe the uncertainty in the model parameters before the data are collected. After the data are collected, a posterior probability distribution is computed via Bayes' theorem. The posterior probability distribution acts as an updated probability distribution for the parameter conditioned on the observed data. Bayesian inference is based on this posterior distribution.

There are many advantages to working under a Bayesian framework. The Bayesian framework, unlike the frequentist framework, does not rely on asymptotic approximations. Asymptotics rely on large sample theory and may not be appropriate in a small sample (number of experiments) setting. Furthermore, the Bayesian framework provides a well developed theory for modeling hierarchical data (e.g., replicates within-experiment, experiments within-study). In contrast, classical frequentist nonlinear mixed-effects models tend to run into convergence problems when the number of random-effect parameters increase.

This chapter introduces the methodology for the proposed Bayesian Hierarchical Nonlinear  $E_{max}$  model / Bayesian Effect Interaction Index method. The Bayesian Hierarchical Nonlinear  $E_{max}$  model / Bayesian Effect Interaction Index method is advantageous in that it accounts for various sources of variation and uncertainty, borrows strength across independently repeated experiments, and allows one to incorporate prior knowledge into the



current analysis, thus offering a more efficient and reliable inference. Extensive simulation studies show that the Bayesian Hierarchical Nonlinear Emax model / Bayesian Effect Interaction Index method provides an improved methodology for making population (group) inference. This chapter is based on the published work “A Bayesian Approach to Dose-Response Assessment and Synergy and Its Application to In Vitro Dose Response Studies”, (Hennessey, Rosner, Bast Jr., Chen, 2010. *Biometrics*).

### 3.2 Introduction

The Median-Effect Principle / Combination Index method (Chou and Talalay, 1984) is the most commonly used method for assessing *in vitro* dose-response and drug-drug interaction. There is a need to improve current standard analysis with the Median-Effect Principle / Combination Index method (MEPCI). MEPCI ignores variation inherent in the data, such as, variation in the controls and variation between repeated experiments. Ignoring these variations can lead to bias and unreliable inferences. Furthermore, standard data preprocessing techniques for application of MEPCI are inefficient. Standard data preprocessing techniques normalize averaged responses by the average control responses which can induce unwanted correlation. Also, if a normalized data point falls outside the allowed  $[0, 1]$  range, the data point is thrown away. In general, throwing away data points is not a good idea; it causes information to be lost. Another issue arises when MEPCI performs hypothesis testing of additivity. The 95% confidence interval is constructed for the combination index (CI); however, the coverage probability of the confidence interval falls below the nominal value of 95% (Boik et al., 2008). This can lead to a high incidence of type I error. Reducing type I errors benefits drug developers by ensuring resources are not allocated to false positives, that is, combined agents that are declared synergistic when in fact they are additive.

We developed a three-stage Bayesian hierarchical nonlinear regression model that accounts for within-experiment variation, between-experiments variation, variation in the controls, and heteroscedasticity. The model consists of a modified Hill's model ( $E_{max}$  model) with an additive residual error on the logarithmic scale. In addition, we developed a Bayesian Effect Interaction Index method that allows one to assess quantitatively interaction between two agents combined at a fixed dose ratio. The Bayesian Effect Interaction Index method performs decision making based on the posterior distribution of the Loewe interaction index and makes honest account of uncertainty in the input parameters of the isobole equation (Loewe's additive model).

### **3.3 Bayesian Hierarchical Nonlinear $E_{max}$ Model / Bayesian Effect Interaction Index Method**

#### **3.3.1 The Model**

The proposed model can be used for a positive continuous response of a single agent or a combination of two agents combined at a fixed dose ratio. In stage 1 of the hierarchical model, we model the intra-experiment variation (variability within-experiment but between replicates). Let  $y_{ijk}$  be a positive continuous measured response for experiment  $i$  replicate  $j$  at the  $k^{\text{th}}$  concentration level  $c_k$ . The data model is

$$\log(y_{ijk}) = \mu_{ik} + \varepsilon_{ijk}$$

with mean response  $\mu_{ik}$  and random error term  $\varepsilon_{ijk} \sim N(0, \sigma^2)$ . The role of the error term is to account for variation beyond what is explained by an agent's concentration level. This includes variation between replicates, measurement error, and the natural variation within a replicate. The log (base  $e$ ) transformation is commonly used for positive data and helps to satisfy the

assumption of constant variance for the error terms. It follows that on the original scale  $\text{Var}(Y_{ijk}) = \sigma^2 \mu_{ik}$  where  $\mu_{ik}$  represents the mean response on the log scale. This implies a non-constant variance (heteroscedasticity) on the original scale across dose levels and across experiments. This heteroscedasticity trend is commonly seen. For other heteroscedascity trends, other error functions may be used (e.g.,  $\sigma^2 \mu_{ik}^\theta$ ).

On the original scale, response follows a modified Hill's equation (Hill, 1910), that is,

$$E(Y_{ijk}) = \frac{E_{0,i}}{1 + \left(\frac{C_k}{IC_{50,i}}\right)^{M_i}}$$

This is the  $E_{max}$  curve with parameters  $E_0$ ,  $IC_{50}$ , and  $M$ . The parameter  $E_0$  represents the expected response in the absence of the drug.  $IC_{50}$  represents the concentration required to inhibit 50% of the cells and  $M$  is a shape parameter known as Hill's coefficient. Variability occurs between independently repeated experiments; therefore, we allow the parameters  $E_0$ ,  $IC_{50}$ , and  $M$  to vary across experiments (indexed by  $i$ ). When fitting the model to data from a combination study (e.g., agent A + agent B) with a fixed dose ratio  $\rho = \text{dose}_B/\text{dose}_A$ , we treat the concentration of A as the independent variable for convenience. Inference can be in terms of agent A or agent B, however, because of  $\rho$ .

In stage 2 of the hierarchical model we model the inter-experiment variation (between-experiment variation). We suggest Log-normal prior distributions for the parameters  $E_0$ ,  $IC_{50}$ , and  $M$ .

Priors:

$$E_{0,i} \sim \text{LogN}(\mu_{\log E_0}, \sigma_{\log E_0}^2)$$

$$IC_{50,i} \sim \text{LogN}(\mu_{\log IC_{50}}, \sigma_{\log IC_{50}}^2)$$

$$M_i \sim \text{LogN}(\mu_{\log M}, \sigma_{\log M}^2)$$

The Log-normal prior distributions ensure positive values and provide a realistic skewness of the parameter distribution. Note that for inhibitory activities,  $M$  is positive.

Bayesian hierarchical models use prior distributions that themselves depend on parameters (hyper-parameters). A reasonable assumption is that each individual experiment arises from a population of experiments. The location hyperparameters,  $\mu_{\log E_0}$ ,  $\mu_{\log IC_{50}}$ , and  $\mu_{\log M}$  represent the population (group) means on the log scale. The scale hyperparameters  $\sigma_{\log E_0}^2$ ,  $\sigma_{\log IC_{50}}^2$ , and  $\sigma_{\log M}^2$  represent the between-experiment parameter variation on the log scale. A prior distribution (hyper-prior) is then required for the hyper-parameters. In the third stage, we complete the hierarchical model by specifying the hyper-priors. We suggest the following hyper-priors to complete the hierarchical model.

Hyper-priors:

$$\mu_{\log E_0} \sim N(a, d), \quad \sigma_{\log E_0} \sim \text{half-Cauchy}(g)$$

$$\mu_{\log IC_{50}} \sim N(b, e), \quad \sigma_{\log IC_{50}} \sim \text{half-Cauchy}(h)$$

$$\mu_{\log M} \sim N(c, f), \quad \sigma_{\log M} \sim \text{half-Cauchy}(l)$$

Normal distributions are used for the location hyperparameters and half-Cauchy distributions for the standard deviation hyperparameters. Historical information may be available for a single-agent's median inhibitory concentration and could be incorporated into the analysis at this stage of the hierarchy (Davidian and Giltinan, 1995). Otherwise, we set  $a$ ,  $b$ , and  $c$  to an arbitrary value (e.g.,  $a = 0$ ,  $b = 0$ , and  $c = 0$ ). We set  $d$ ,  $e$ , and  $f$  to reflect vague (flat) priors (e.g.,  $d = 1000$ ,  $e = 1000$ , and  $f = 1000$ ).

Choosing a hyper-prior distribution for the scale hyper-parameters  $\sigma_{\log E_0}$ ,  $\sigma_{\log IC_{50}}$ , and  $\sigma_{\log M}$  can be an important step. It is common practice to use an Inverse-Gamma hyper-prior distribution for the variance ( $\sigma^2$ ) hyper-parameters or a Uniform hyper-prior distribution for standard deviation ( $\sigma$ ) hyper-parameters. Gelman (2006) showed that excessive-shrinkage and

under-shrinkage can be a problem in Bayesian hierarchical models when using these hyper-prior distributions, especially when the number of groups (e.g., experiments) is small. Shrinkage is the pulling of second-level parameter estimates towards the overall mean.

Gelman (2006) showed the half-Cauchy to have some nice properties. The half-Cauchy distribution is characterized by non-negative quantities, a broad peak at 0, and a fatter tail than that of a Normal distribution. Gelman (2006) proposed half-Cauchy hyper-prior distributions for standard deviation hyper-parameters when the number of groups is less than eight. Using the half-Cauchy distribution involves re-parameterizing for the parameters  $E_{0,i}$ ,  $IC_{50,i}$ , and  $M_i$ . Below we show the reparametrization for  $IC_{50}$ . There is a similar reparameterization for  $E_{0,i}$  and  $M_i$ .

$$\begin{aligned}
IC_{50,i} &\sim \text{LogN}(\theta_{i,\log IC_{50}}, \sigma_{\log IC_{50}}^2) \\
\theta_{i,\log IC_{50}} &= \mu_{\log IC_{50}} + \xi_{\log IC_{50}} * \eta_{i,\log IC_{50}} \\
\xi_{\log IC_{50}} &\sim N(0, h^2), \quad \eta_{i,\log IC_{50}} \sim N(0, \tau_{\eta_{\log IC_{50}}}^{-1}) \\
\tau_{\eta_{\log IC_{50}}} &\sim \text{Gamma}(0.5, 0.5) \\
\sigma_{\log IC_{50}} &= \frac{|\xi_{\log IC_{50}}|}{\sqrt{\tau_{\eta_{\log IC_{50}}}}}
\end{aligned}$$

The reparametrization improves Markov chain Monte Carlo (MCMC) convergence by reducing dependence among the parameters in the hierarchical model (Gelman, 2006). Gelman recommends a value for  $h$  that reflects a weakly informative prior.

### 3.3.2 Bayesian Posterior Inference

One may use Markov Chain Monte Carlo (MCMC) via WinBUGS (Spiegelhalter, 2002) to simulate samples from posterior distributions of relevant parameters. Interest lies in

making population (group) level inference.

### 3.3.2.1 Dose-Response Assessment

In dose-response assessment, a quantity of interest is the inhibitory concentration ( $IC_x$  = the concentration producing  $x\%$  inhibition). Posterior estimates of  $IC_x$  require a function of the parameters from the fitted Bayesian hierarchical nonlinear  $E_{max}$  model. Population level inference requires parameters from Stage 3 of the hierarchical model. For example, the  $g^{th}$  posterior sample of  $IC_x$  at the population level is constructed by the following inverse function where the outcome is  $(1-Y/E_0)$ :

$$IC_x^{(i)} = \mu_{IC_{50}}^{(i)} \left( \frac{x}{100 - x} \right)^{1/\mu_M^{(i)}} \quad (3.1)$$

The superscript ( $i = 1, \dots, N$ ) refers to saved MCMC samples where  $N$  is the number of MCMC samples used for posterior inference. The Bayesian framework provides a straightforward method for propagation of uncertainty; that is, the uncertainty in  $\mu_{IC_{50}}$  and  $\mu_M$  will propagate into uncertainty about  $IC_x$ . Informative summary statistics of  $IC_x$  can include the median and the Bayesian 95% credible interval. The Bayesian 95% credible interval is constructed with the 2.5 percentile and the 97.5 percentile and can be interpreted as an interval within which the parameter  $IC_x$  lies with probability 0.95.

A population mean dose-response curve can be displayed graphically by using equation (1.2) with exponentiated posterior estimates of  $\mu_{E_0}$ ,  $\mu_{IC_{50}}$ , and  $\mu_M$ . A median-fitted response is recommended on the original scale because of skewness.

### 3.3.2.2 Drug-Drug Interaction Analysis

In drug-drug interaction analysis, one quantitatively assesses the interaction (additivity, synergism, antagonism) between two agents at different inhibitory levels. The proposed

Bayesian Hierarchical Nonlinear Emax model / Bayesian Effect Interaction Index method (Hennessey et al., 2010) integrates results from the single agents and the combined agents' fitted curves and computes a posterior distribution for Loewe interaction index at a specific inhibitory level. For example, posterior samples of Loewe interaction index at inhibitory level  $x\%$  ( $II_x$ ) are constructed by the following function, also known as the isobole equation

$$II_x^{(i)} = \frac{IC_{x,A+B}^{(i)}}{IC_{x,A}^{(i)}} + \frac{\rho * IC_{x,A+B}^{(i)}}{IC_{x,B}^{(i)}}. \quad (3.2)$$

In the numerators,  $IC_{x,A+B}$  represents the concentration of agent A in the combination (agent A + agent B) yielding  $x\%$  inhibition;  $\rho = \text{dose}_B/\text{dose}_A$  is the fixed dose ratio used in the combination study. In the denominators,  $IC_{x,A}$  and  $IC_{x,B}$  represent the inhibitory concentrations of agent A alone and agent B alone, respectively, that yields the same  $x\%$  inhibition. Here, the input parameters are considered random, and posterior estimates are generated using the method described in Section 3.3.2.1.

The Bayesian Effect Interaction Index method performs decision making based on the posterior distribution of  $II_x$ . The decision rule is to conclude synergy (antagonism) if  $II_x$  falls below (lies above) one with high probability. Additivity is concluded in the absence of synergy or antagonism. The posterior probability that  $II_x$  falls below 1 is calculated by

$$\gamma = \Pr(II_x < 1 - \epsilon | \text{data}) \cong \frac{1}{N} \sum_{i=1}^N \mathbf{I}[II_x^{(i)} < 1 - \epsilon]. \quad (3.3)$$

Here  $\mathbf{I}[\cdot]$  in equation (3.3) is an indicator function. We use  $1 - \epsilon$ , for some small positive  $\epsilon$  (e.g., 0.05), rather than 1, to differentiate synergy from additivity in case  $II_x$  is close to 1. We conclude synergy if  $\gamma$  exceeds some threshold. For example, we declare "Synergy" if  $\gamma > 0.80$ . The threshold 0.80 is chosen based on prior work (Hennessey et al., 2010) that showed a threshold of 0.80 had good operating characteristics. Other threshold values that may be

considered are 0.90 or 0.70. The threshold used may be context specific but ultimately one would want a threshold that minimizes error and maximizes correct decision making.

If interest is in additive agents, the posterior probability that  $II_x$  lies above 1 is also calculated.

$$\lambda = \Pr(II_x > 1 + \epsilon | data) \cong \frac{1}{N} \sum_{i=1}^N \mathbf{I} \left[ II_x^{(i)} > 1 + \epsilon \right] \quad (3.4)$$

We declare "Antagonism" if  $\lambda > 0.80$ , "Synergy" if  $\gamma > 0.80$ , else "Additivity" is declared.

### 3.4 Simulation Study

We conducted a simulation study to evaluate and compare the performance of our proposed Bayesian Hierarchical Nonlinear  $E_{max}$  Model / Bayesian Effect Interaction Index method to meta-analysis with the Median-Effect Principle / Combination Index method. We also investigated the effect of sample size on performance.

First, dose-response data for three hypothetical agents were generated: agent A, agent B, and agent A + agent B. For each hypothetical agent, dose-response data from an  $E_{max}$  model was generated. An  $E_{max}$  model was used instead of the Median-Effect equation so we could introduce variation in the controls. Each realization included ten concentration levels (with serial 2-fold changes) and three (or six) independent experiments. Each experiment contained three replicates per dose level, yielding 30 observations per experiment and 90 (or 180) observations per realization. We introduced the following variation in the generated data: variation within-experiment (between-replicates), variation between-experiments, variation in the responses of the controls, and heteroscedasticity. All variations were set to values similar to those observed in the real data.

Table 3.1 contains parameter values used for generating the simulation data. For hypothetical agent A, the "true" population mean curve is  $Y = 3/(1+(C/10)^{1.49})$ . This is an  $E_{max}$



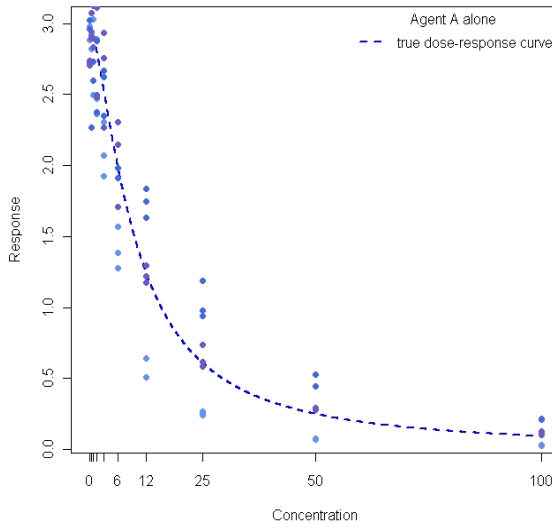
**Table 3.1. Parameter values used for generating simulation data.** The simulation considers three hypothetical agents: Agent A alone, Agent B alone, and Agent A + Agent B (combined at a fixed dose ratio  $\rho = 0.055$ ).

	Agent A alone	Agent B alone	Agent A+Agent B
$E(Y) = E_0/[1+(C/IC_{50})^M]$	$3/[1+(C/10)^{1.49}]$	$3/[1+(C/1.38)^{1.37}]$	$3/[1+(C/0.69)^{0.67}]$
within-experiment noise ( $\sigma^2$ )	0.010	0.010	0.0100
between-experiment noise for $E_0$ ( $\sigma_{E_0}^2$ )	0.020	0.020	0.0200
between-experiment noise for $IC_{50}$ ( $\sigma_{IC_{50}}^2$ )	16.0000	0.300	0.0700
between-experiment noise for $M$ ( $\sigma_M^2$ )	0.018	0.015	0.0036
concentrations ( $\mu M$ )	(0, 0.39, 0.78, 1.56, 3.125, 6.25, 12.5, 25, 50, 100)	(0, 0.125, 0.25, 0.5, 1, 2, 4, 8, 16, 32)	(0, 1, 2.05, 4.1, 8.2, 16.4, 32.8, 65.6, 131.2, 262.4)

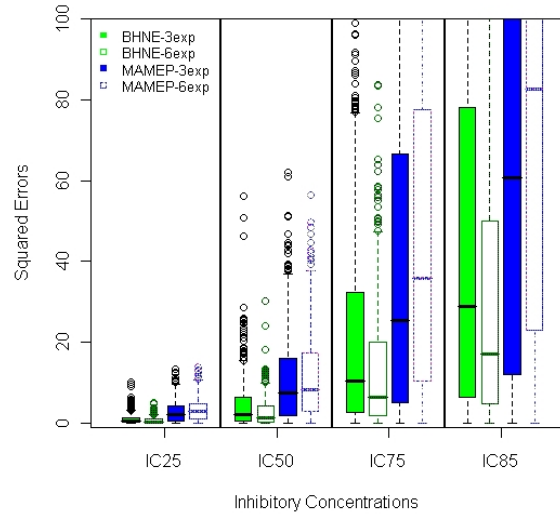
model with parameter values  $E_0 = 3$ ,  $IC_{50} = 10$ , and  $M = 1.49$ . With the idea that experiment-specific curves deviate from the true population mean curve and replicates within-experiment deviate from their experiment-specific mean curve, we proceed with the following: sample experiment-specific  $E_{0,i}$  from a log-normal distribution to constrain values to be positive; sample  $IC_{50,i}$  and  $M_i$  from a bivariate log-normal distribution to constrain positive values and to introduce plausible correlation between the two parameters; use a multiplicative error term to ensure positive data points and introduce heteroscedasticity; set the within-experiment variation to  $\sigma^2 = 0.01$ ; set the between-experiment parameter variation for  $IC_{50}$  to  $\sigma_{IC_{50}}^2 = 16$ ; and allow for minimal variation between-experiments in the controls and the shapes of the curves represented by  $\sigma_{E_0}^2 = 0.02$  and  $\sigma_M^2 = 0.018$ . The same procedure is applied for hypothetical agent B and hypothetical agent A + agent B, with the exception that we use different parameter values and different between-experiments parameter variation.

Figures 3.1(a), 3.2(a), and 3.3(a) display the true curves with one realization from the simulated data for hypothetical agent A, hypothetical agent B, and hypothetical agent A + agent B, respectively. Realizations with three experiments are displayed but we also investigated realizations with six experiments to see the effect of increasing the number of experiments. Figures 3.1(b), 3.2(b), and 3.3(b) display the distributions of the squared errors in estimating population level  $IC_{25}$ ,  $IC_{50}$ ,  $IC_{75}$ , and  $IC_{85}$  with fitted Bayesian Hierarchical  $E_{max}$  model (green boxplots) and meta-analysis Median-Effect Principle (blue boxplots). The color filled boxplots are used when three experiments per realization are considered. The color outlined boxplots are used when six experiments per realization are considered.

From Figures 3.1(b), 3.2(b), and 3.3(b), we conclude that the Bayesian Hierarchical Nonlinear  $E_{max}$  model provides a more precise estimator for  $IC_{25}$ ,  $IC_{50}$ ,  $IC_{75}$ , and  $IC_{85}$  compared to meta-analysis with Median-Effect Principle. Precision is evaluated by the distribution of the

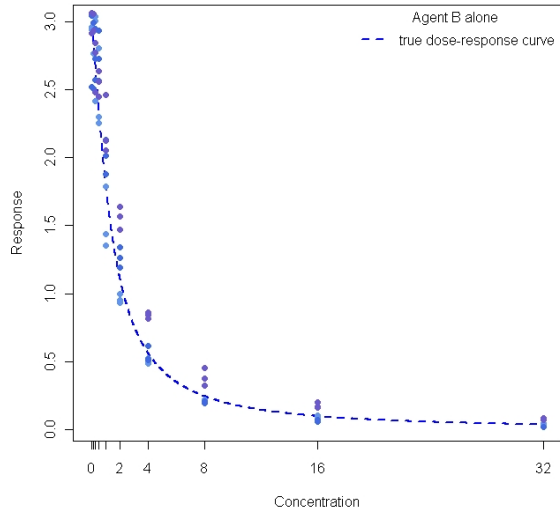


(a)

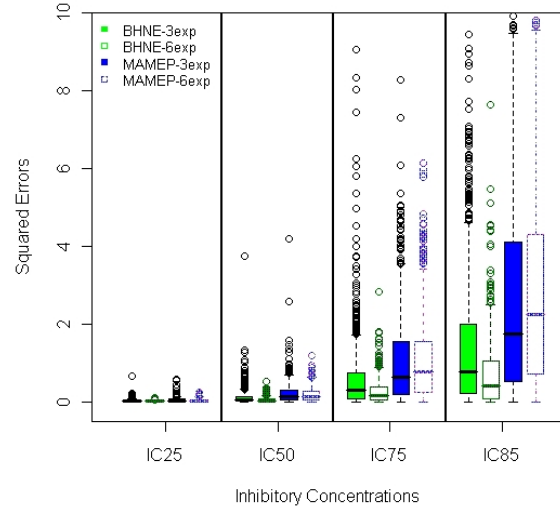


(b)

**Figure 3.1 Simulation results for hypothetical agent A.** (a) The simulation truth is  $Y = 3 / [1+(C/10)^{3/2}]$ . The blue dashed curve represents the simulation truth for hypothetical agent A and the points represent one realization from the simulated data. (b) The distributions of the squared errors in estimating inhibitory concentrations with fitted Bayesian Hierarchical Nonlinear  $E_{max}$  model (BHNE) and meta-analysis Median-Effect Principle (MAMEP). The color filled boxplots represent when three experiments per realization are considered. The color outlined boxplots represent when six experiments per realization are considered.



(a)



(b)

**Figure 3.2 Simulation results for hypothetical agent B.** (a) The simulation truth is  $Y = 3 / [1+(C/1.38)^{1.37}]$ . The blue dashed curve represents the simulation truth for hypothetical agent B and the points represent one realization from the simulated data. (b) The distributions of the squared errors in estimating inhibitory concentrations with fitted Bayesian Hierarchical Nonlinear  $E_{max}$  model (BHNE) and meta-analysis Median-Effect Principle (MAMEP). The color filled boxplots represent when three experiments per realization are considered. The color outlined boxplots represent when six experiments per realization are considered.

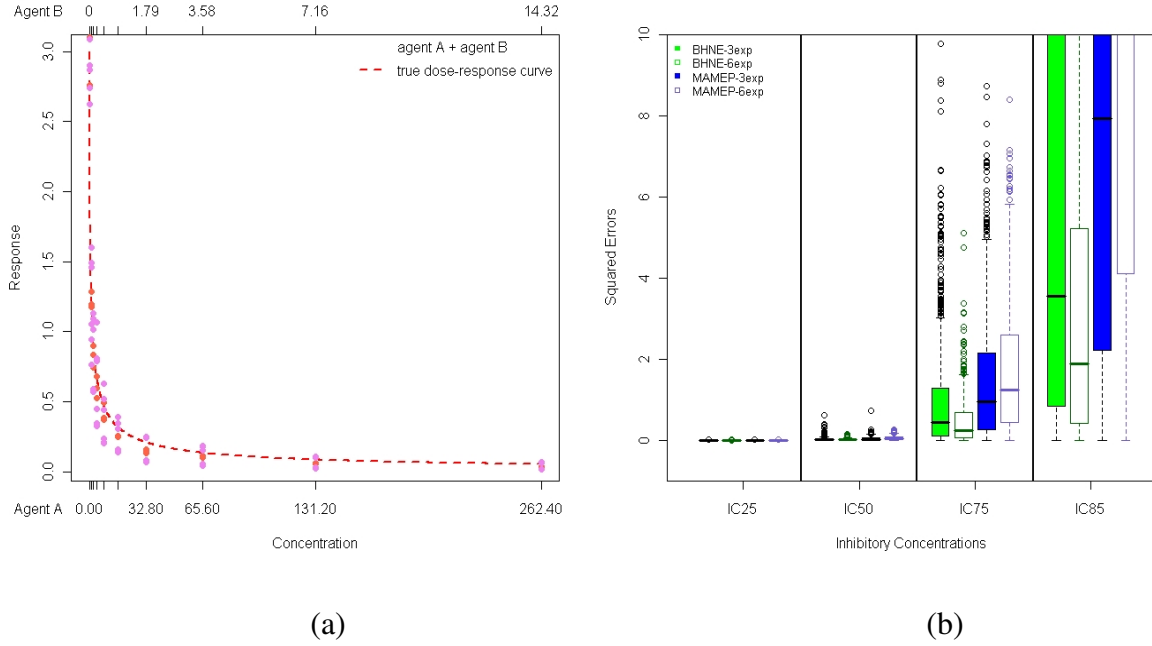


**Figure 3.3 Simulation results for hypothetical agent A + agent B.** The simulation truth is  $Y = 3 / [1 + (C/0.69)^{0.67}]$ . The red dashed curve represents the simulation truth for hypothetical agent A and the points represent one realization from the simulated data. (b) The distributions of the squared errors in estimating inhibitory concentrations with fitted Bayesian Hierarchical Nonlinear  $E_{max}$  model (BHNE) and meta-analysis with the Median-Effect Principle (MAMEP). The color filled boxplots represent when three experiments per realization are considered. The color outlined boxplots represent when six experiments per realization are considered.

squared errors. Performance decreases with increasing inhibitory levels, but the Median-Effect Principle's performance tends to decrease at a higher rate compared to the Bayesian Hierarchical Nonlinear  $E_{max}$  model. For the Bayesian Hierarchical Nonlinear  $E_{max}$  model, we find that increasing the sample size from three to six experiments reduces the median squared error. In some cases, the median-squared error was reduced by as much as 50%. This was not observed with the meta-analysis Median-Effect Principle; estimator performance did not improve with increasing sample size, suggesting that meta-analysis with the Median-Effect Principle does not provide a consistent estimator.

In conclusion, performance depends on a lot of factors including sample size, the magnitude of variation between experiments, inhibitory level, and if the parameter estimate lie in a flat region of the dose-response curve. Overall, the Bayesian Hierarchical Nonlinear  $E_{max}$  model provides a more reliable estimator of the population level dose-response curve.

We also investigated the performance of the Bayesian Effect Interaction Index method in drug-drug interaction analysis. Three drug interaction scenarios were considered. In scenario 1, agent B is combined with itself (a sham experiment). By definition, an agent cannot interact with itself and additivity should be concluded at all inhibitory levels. In scenario 2, agent A is combined with agent B producing strong synergy across all inhibitory levels. In scenario 3, agent A is combined with agent B producing qualitatively changing interaction, that is, strong synergy at 5% inhibition to very strong antagonism at 95% inhibition.

Figure 3.4 (a) shows the simulation results for scenario 1 (sham experiment) when three experiments are considered. Figure 3.4(b) shows the results when six experiments are considered. Plotted are the percentages of the 1000 realizations that additivity was correctly declared. Overall, the Bayesian Effect Interaction Index with thresholds  $\gamma > 0.90$  performed well under a sham experiment scenario. Meta-analysis with Median-Effect Principle /

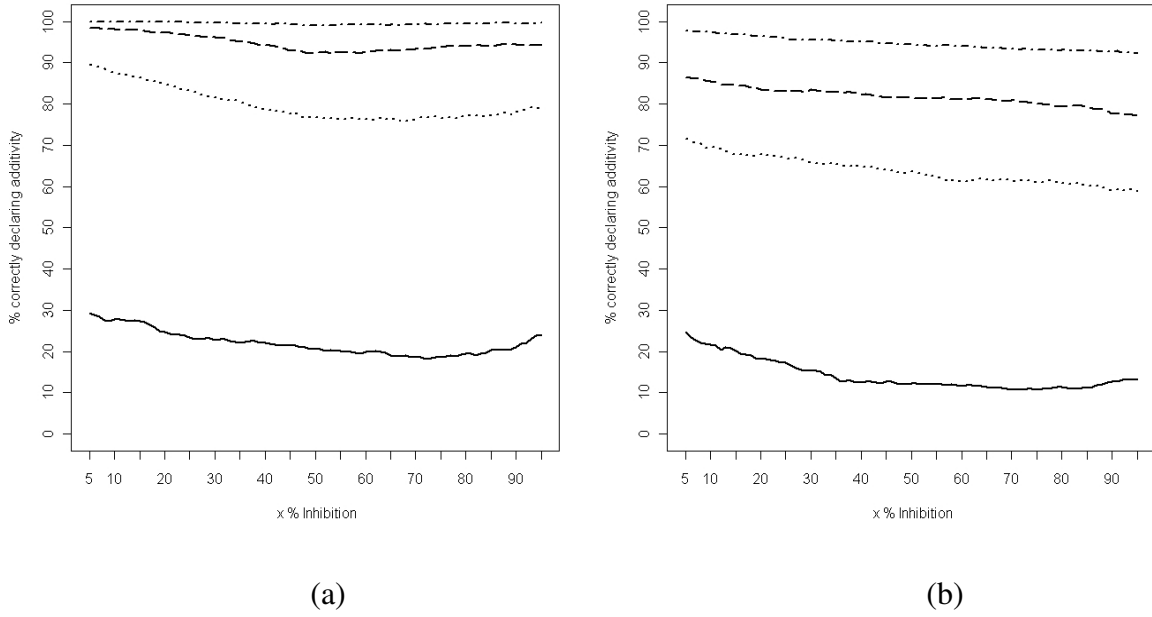


**Figure 3.4 Simulation results for drug interaction scenario 1, agent B combined with itself (sham experiment).** The simulation truth is that the interaction index has a value of one across all inhibitory levels and additivity should be concluded at all inhibitory levels. Plotted are the percentages of the 1000 realizations that additivity was correctly declared. Solid line: meta-analysis Median-Effect Principle / Combination Index method. Dash-dot line: Bayesian hierarchical nonlinear  $E_{max}$  model / Bayesian Effect Interaction Index method using  $\gamma > 0.90$  and  $\epsilon = 0.05$ . Dashed line: Bayesian hierarchical nonlinear  $E_{max}$  model / Bayesian Effect Interaction Index method using  $\gamma > 0.80$ . Dot line: Bayesian hierarchical nonlinear  $E_{max}$  model / Bayesian Effect Interaction Index method using  $\gamma > 0.70$ . (a) 3 experiments are considered per realization. (b) 6 experiments are considered per realization.

Combination Index method led to a high risk of type I error, that is, erroneously rejecting additivity when in fact additivity is true.

Figures 3.5(a) and 3.5(b) show the simulation results for scenario 2 (strong synergy across all inhibitory levels) when three experiments and six experiments, respectively, are considered. The Combination Index method and the Bayesian Effect Interaction Index method with  $\gamma > 0.80$  and  $\gamma > 0.70$  performed well under a strong synergy scenario; both methods had high rates of correctly declaring synergy. The Bayesian Effect Interaction Index method performed slightly worse when inhibition was close to 0% or 100% (i.e., a large fraction of the cells are alive or dead). This is rectified by increasing the number of experiments from three to six.

Figures 3.6(a) and 3.6(b) show the simulation results for the more problematic scenario, qualitatively changing interaction. The Median-Effect Principle / Combination Index method exhibits low power to detect synergy at most inhibitory levels. The Bayesian Effect Interaction Index method with  $\gamma > 0.80$  and  $\gamma > 0.70$ , correctly declared synergy most of the time. The exception is when there are quick changes in the interaction index values and interaction is changing qualitatively (i.e., synergistic to additive to antagonism). Increasing the number of experiments from three to six improved performance over a larger range of inhibitory levels.

In summary, we conclude that the Bayesian Effect Interaction Index method with  $\gamma > 0.80$  maintained good operating characteristics.

### 3.5 Application to the Ovarian Cancer Cell Lines Study

We apply the Bayesian Hierarchical Nonlinear  $E_{max}$  Model/Bayesian Effect Interaction Index method to real data from the ovarian cancer cell line study. We present, in detail, dose-response assessment of the cell line HEY treated with DAC alone, SAHA alone, and a comb-



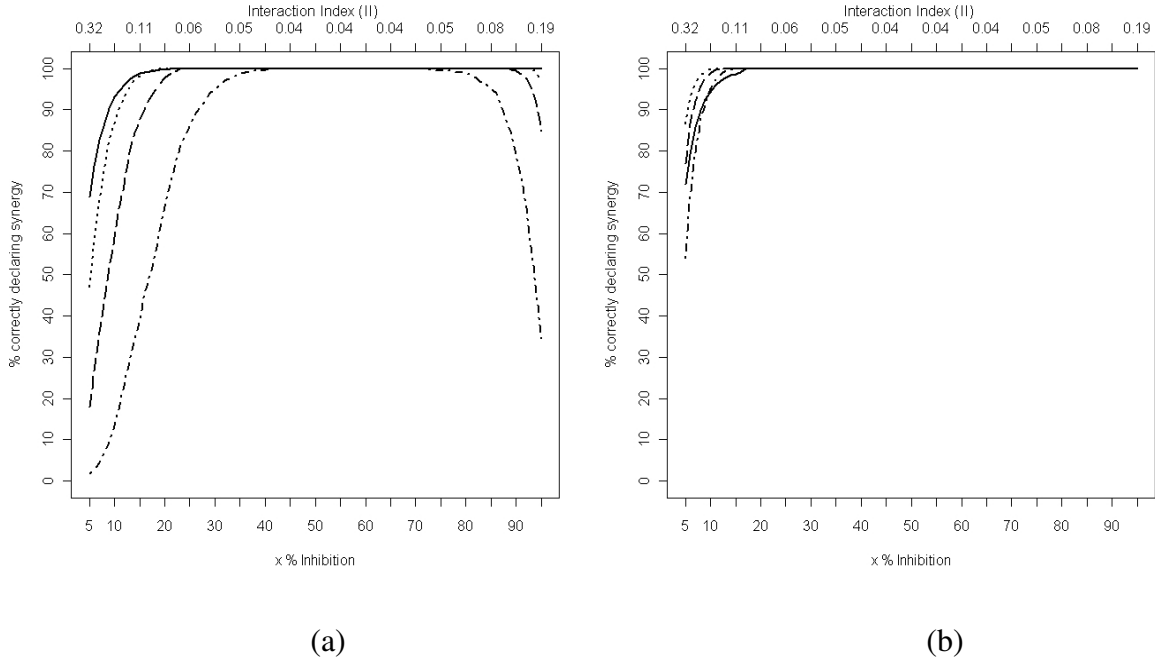


**Figure 3.5 Simulation results for drug interaction scenario 2, agent A combined with agent B produces strong synergy.** The simulation truth is that the interaction index has a value less than one across all inhibitory levels. True values are shown on top axis. Plotted are the percentages of the 1000 realizations that synergy was correctly declared. Solid line: meta-analysis Median-Effect Principle / Combination Index method. Dash-dot line: Bayesian hierarchical nonlinear  $E_{max}$  model / Bayesian Effect Interaction Index method using  $\gamma > 0.90$ . Dashed line: Bayesian hierarchical nonlinear  $E_{max}$  model / Bayesian Effect Interaction Index method using  $\gamma > 0.80$ . Dot line: Bayesian hierarchical nonlinear  $E_{max}$  model / Bayesian Effect Interaction Index method using  $\gamma > 0.80$ . (a) 3 experiments are considered per realization. (b) 6 experiments are considered per realization.

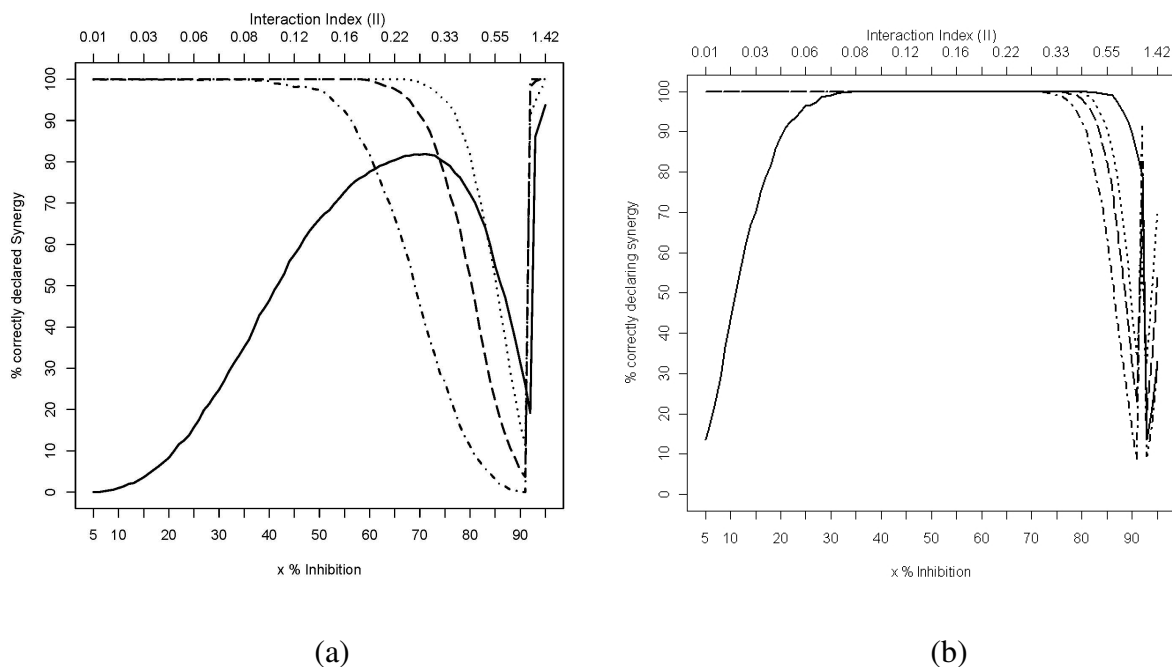


**Figure 3.6 Simulation results for drug interaction scenario 3, agent A combined with agent B produces qualitatively changing interaction.** True interaction index values are shown on top axis. The interaction index values are shown on a grid of  $x$  % inhibitory levels. Plotted are the percentages of the 1000 realizations that synergy (or no synergy) was correctly declared. Solid line: meta-analysis Median-Effect Principle / Combination Index method. Dash-dot line: Bayesian hierarchical nonlinear  $E_{max}$  model / Bayesian Effect Interaction Index method using  $\gamma > 0.90$ . Dashed line: Bayesian hierarchical nonlinear  $E_{max}$  model / Bayesian Effect Interaction Index method using  $\gamma > 0.80$ . Dot line: Bayesian hierarchical nonlinear  $E_{max}$  model / Bayesian Effect Interaction Index method using  $\gamma > 0.80$ . (a) 3 experiments are considered per realization. (b) 6 experiments are considered per realization.

ination of the two agents. For each agent, ten dose levels are investigated. The investigating dose levels range from 0 to 100  $\mu\text{M}$  for DAC alone and 0 to 32  $\mu\text{M}$  for SAHA alone. When combining the agents, DAC concentrations ranged from 0 to 262.40  $\mu\text{M}$ , and SAHA concentrations were 0.055 times the DAC concentrations. The value 0.055 arose from prior findings of the ratio of each agent's estimated median inhibitory concentration ( $p = 0.05$ ). We also provide drug-drug interaction analysis for all agents combined in the ovarian cancer cell line study.

### 3.5.1 Dose-Response Assessment

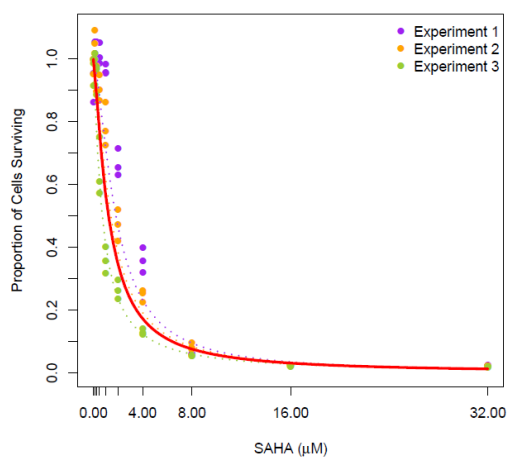
We fit a separate model to each agent's dose-response data. For example, for SAHA alone, we set  $a$ ,  $b$ , and  $c$  to an arbitrary 0 value. We set  $d = 1000$ ,  $e=1000$ , and  $f = 1000$  to reflect vague priors. We set  $g = 5$ ,  $h = 5$ , and  $l = 5$  to reflect weakly informative priors. We made use of WinBUGS (Spiegelhalter, 2002) to perform the MCMC algorithm. The MCMC algorithm simulates samples from the posterior distribution of relevant parameters. This allows us to carry out posterior inference. We ran 30,000 MCMC iterations (three chain run with different initial values) with a thinning factor of 10 to reduce autocorrelation. We discarded the first 20,000 iterations (burn-in) to ensure that the samples are drawn from a stationary distribution. Besides making a visual assessment of goodness of fit, we assessed convergence from the trace plots the 3-chains with different initial values. We then plotted histograms of the posterior samples with their respective prior distributions to ensure the priors were not constraining posterior inferences. For the most part the values chosen for  $a$ ,  $b$ ,  $c$ ,  $d$ ,  $e$ ,  $f$ ,  $g$ ,  $h$ , and  $l$  seem to be reasonable parameter values. The priors do not seem to be constraining posterior inference and there is no significant heavy tails in the posterior distribution to be concern about.

The fitted dose-response curves for SAHA alone, DAC alone, and DAC combined with SAHA are shown in Figure 3.7. The dotted lines represent the experiment-specific fitted curves. The population level model is represented by the solid red line. As expected the population model falls between the experiment-specific fitted curves, providing a meta-analysis of the three experiments. Table 3.2 lists posterior medians and 95% credible intervals for  $IC_{25}$ ,  $IC_{50}$ , and  $IC_{75}$  at the experiment level and at the population level. We note that interval estimates tended to be wide at the population level, because of the large uncertainty with only three experiments. Increasing the number of experiments would narrow our uncertainty at the population level; otherwise we recommend the use of the median, a more robust estimator for the parameters.

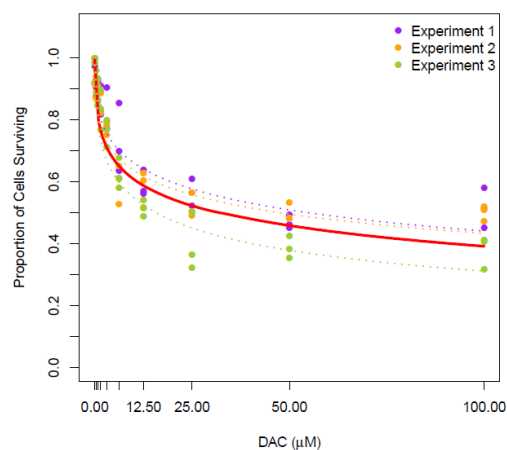
### 3.5.2 Assessment of Synergy

Figure 3.8 and Figure 3.9 shows population posterior predicted dose-effect curves for each combination studies and the respective single agent studies in the cell line HEY and cell line SKOV3. Figure 3.10 and Figure 3.11 displays results from drug-drug interaction analysis for cell lines HEY and SKOV3, respectively. We graphically display results by plotting the posterior distributions of the Loewe interaction index ( $II_x$ ) as boxplots by level of inhibition ( $x$  %). Asterisks indicate inhibitory levels where  $II_x$  fell below 0.95 with high probability ( $\gamma > 0.80$ ).

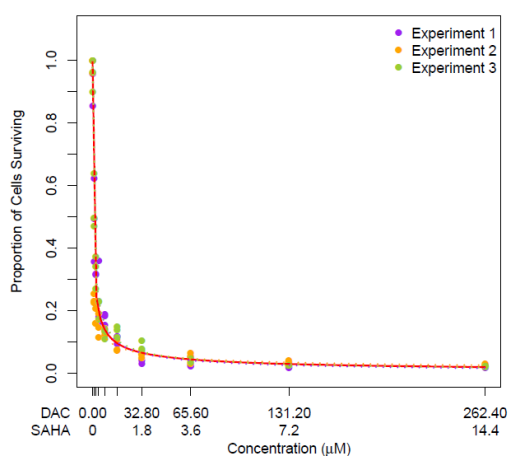
For the cell line HEY, synergy is concluded for DAC+SAHA at inhibitory levels 10-90%. Synergy is concluded for DAC+TSA at inhibitory levels 15-85%. For the cell line SKOV3, synergy is concluded for DAC+SAHA at inhibitory levels 5-60%. Synergy is concluded for DAC+TSA at inhibitory levels 10-55%.



(a) SAHA alone



(b) DAC alone

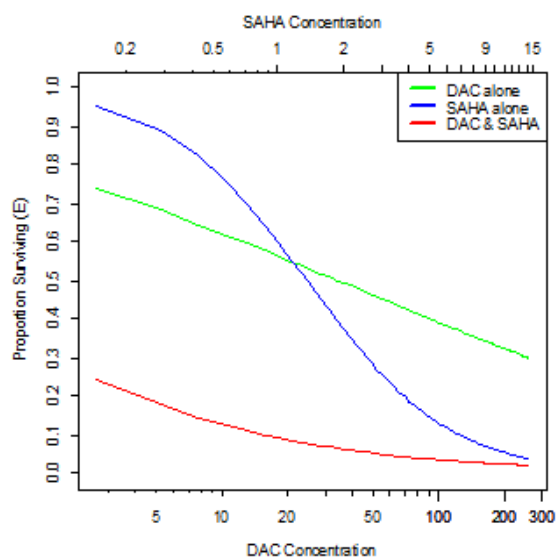


(c) DAC + SAHA

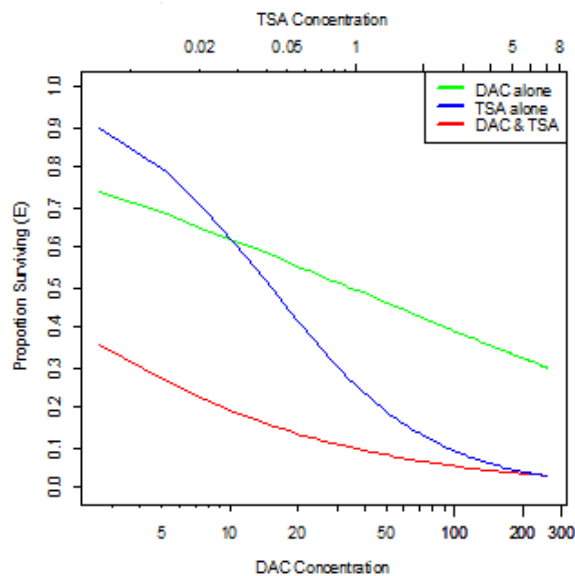
**Figure 3.7 Fitted dose-response curves for DAC and SAHA, alone and combined, in cell line HEY.** Experiment-specific observations are normalized with respect to their observed maximal control response. The fitted curves are normalized with respect to their fitted control effect. The dotted curves represent experiment-specific fits and the solid red lines represent the population level models.

**Table 3.2. Estimates of inhibitory concentrations for DAC alone, SAHA alone, and DAC+SAHA ( $p = 0.055$ ) in cell line HEY.** Posterior medians and 95% credible intervals are provided for inhibitory concentrations at the experiment-specific and population level.

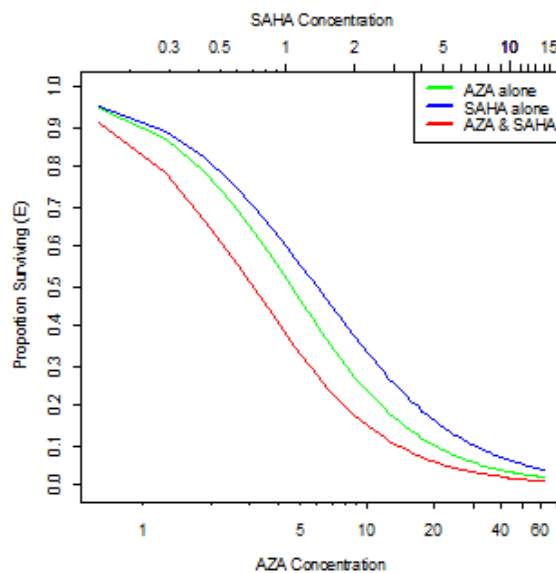
parameter		DAC alone	SAHA alone	DAC+SAHA
IC25	experiment 1	3.46 (1.09, 8.35)	0.89 (0.63, 1.21)	0.15 (0.07, 0.29)
	experiment 2	2.35 (0.61, 6.15)	0.64 (0.44, 0.92)	0.009 (0.002, 0.035)
	experiment 3	1.21 (0.49, 2.78)	0.27 (0.16, 0.44)	0.13 (0.05, 0.27)
	population level	2.12 (0.006, 55.5)	0.53 (0.01, 5.57)	0.05 (2.1E-5, 3.3)
IC50	experiment 1	55.98 (1.09, 8.35)	1.82 (1.39, 2.32)	0.71 (0.36, 1.24)
	experiment 2	48.23 (0.61, 6.15)	1.41 (1.05, 1.90)	0.01 (0.03, 0.30)
	experiment 3	15.77 (0.49, 2.78)	0.71 (0.45, 1.05)	0.68 (0.35, 1.24)
	population level	34.81 (1.72, 773.6)	1.23 (0.11, 12.58)	0.37 (0.007, 19.31)
IC75	experiment 1	894.1 (454.7, 2.4E3)	3.74 (3.04, 4.51)	3.44 (1.95, 5.44)
	experiment 2	996.7 (484.5, 2.9E3)	3.13 (2.49, 3.94)	1.04 (0.46, 0.035)
	experiment 3	203.5 (132.37, 342.74)	1.86 (1.30, 2.51)	3.51 (2.02, 5.80)
	population level	574.7 (21.59, 1.5E5)	2.83 (0.25, 95.91)	2.44 (0.04, 5.9E3)



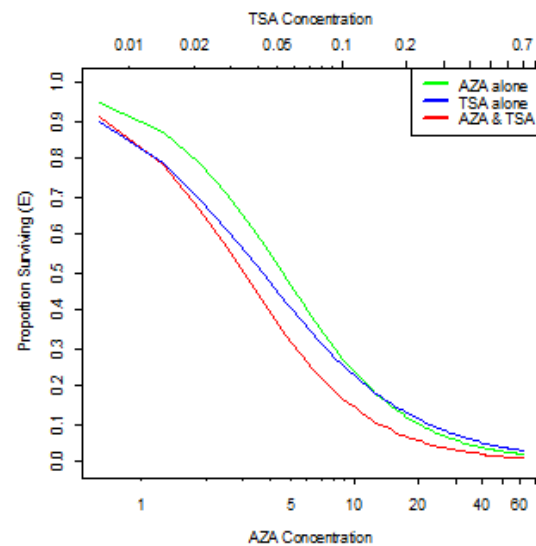
(a) DAC + SAHA



(b) DAC + TSA

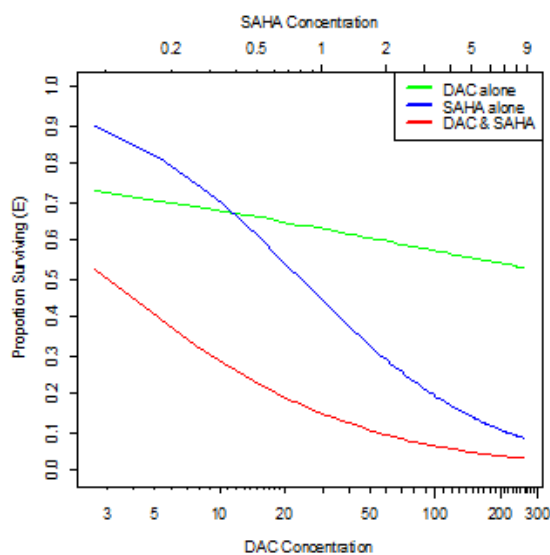


(c) AZA + SAHA

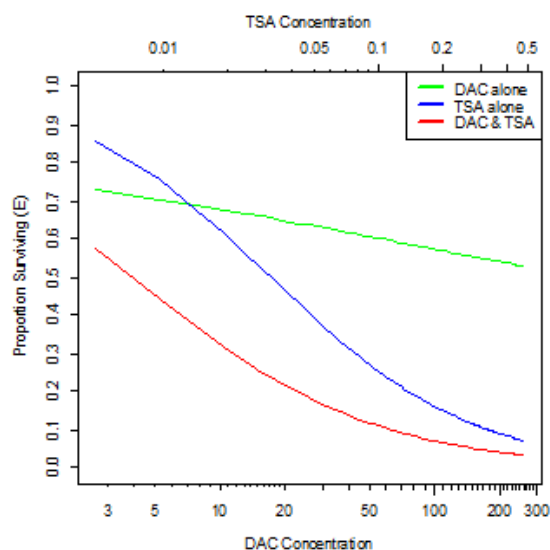


(b) AZA + TSA

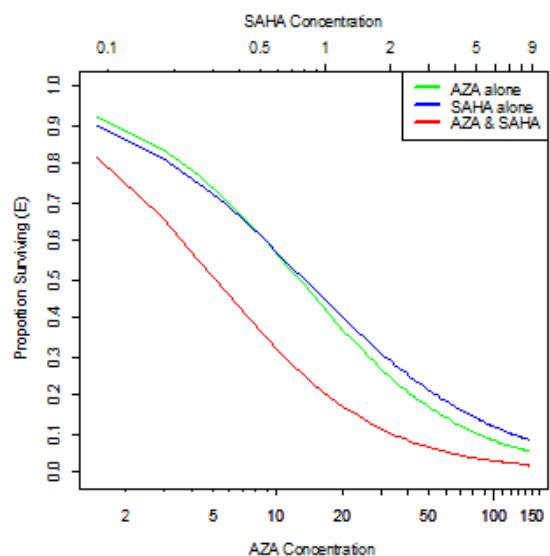
**Figure 3.8** Population level dose response curves for combined agents and their respective single-agents in the cell line HEY. Population level curves for each combination and their respective agents alone. Concentrations are shown on the log scale with labels on the original scale.



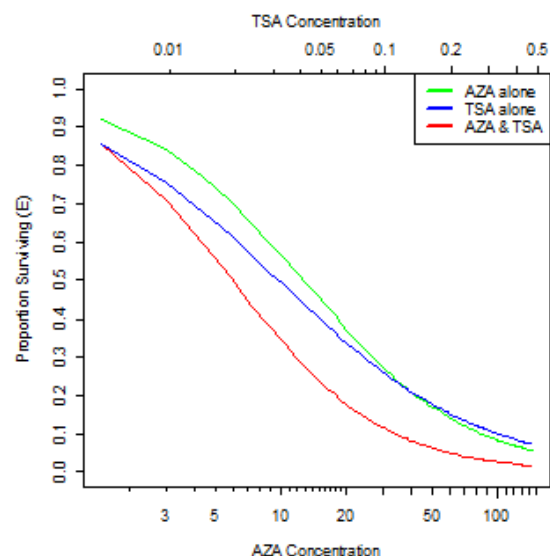
(a) DAC + SAHA



(b) DAC + TSA



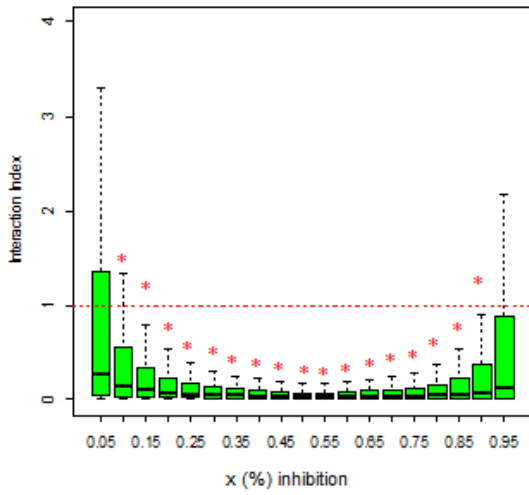
(c) AZA + SAHA



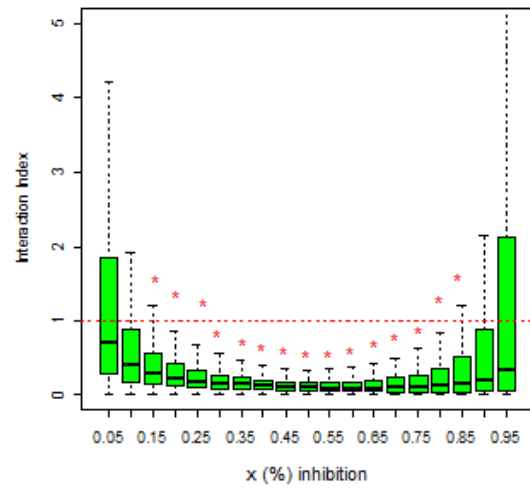
(b) AZA + TSA

**Figure 3.9** Population level dose response curves for combined agents and their respective single-agents in the cell line SKOV3. Population level curves for each combination and their respective agents alone. Concentrations are shown on the log scale with labels on the original scale.

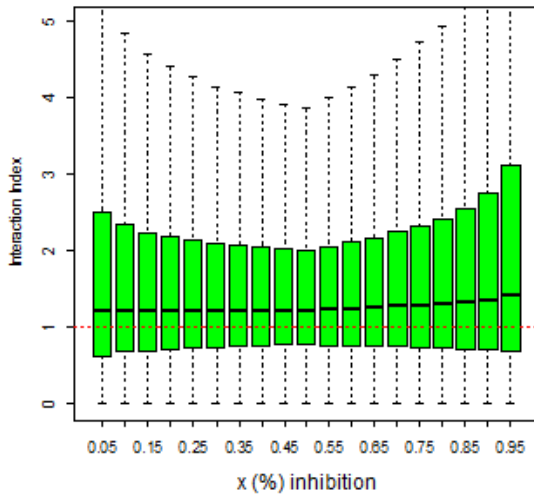




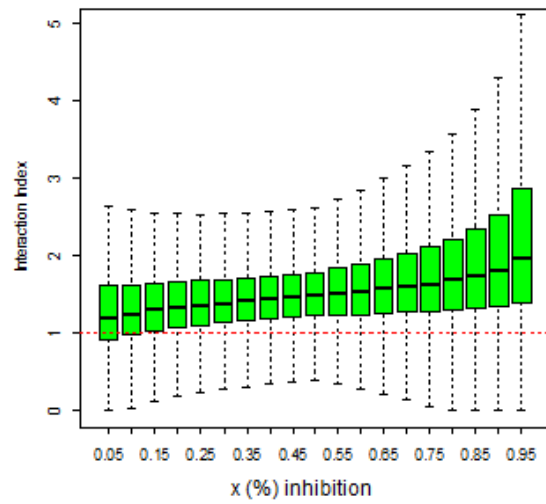
(a) DAC + SAHA



(b) DAC + TSA

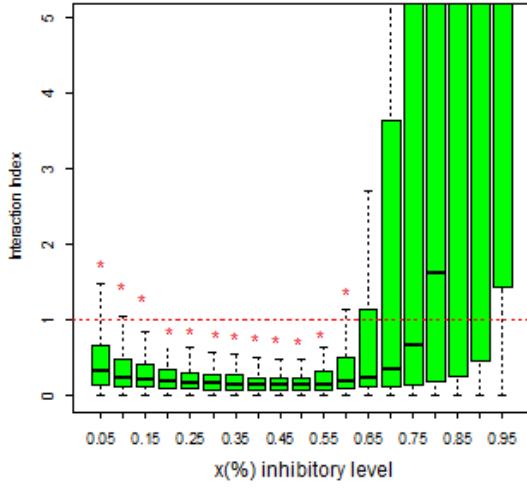


(c) AZA + SAHA

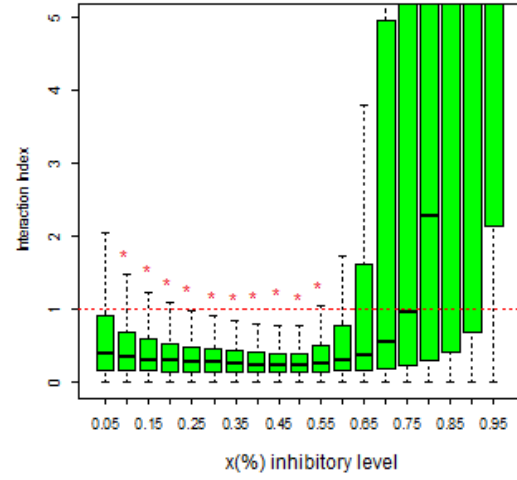


(d) AZA + TSA

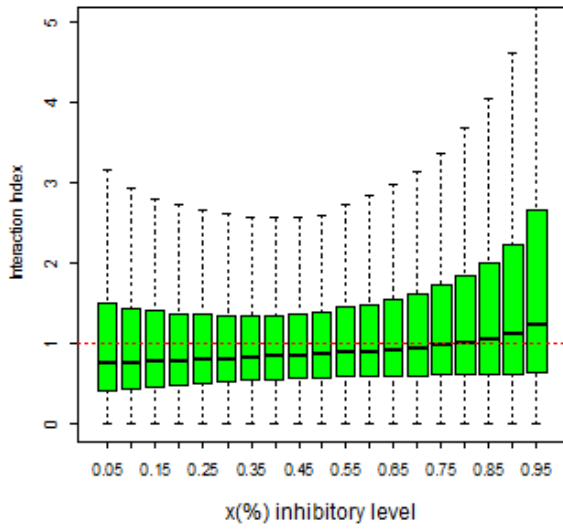
**Figure 3.10** Boxplots of the posterior distributions of Loewe Interaction Index versus inhibitory level in cell line HEY. Asterisks indicate effect levels where  $II_x$  falls below 0.95  $(1-\epsilon)$  with high probability ( $\gamma > 0.80$ ).



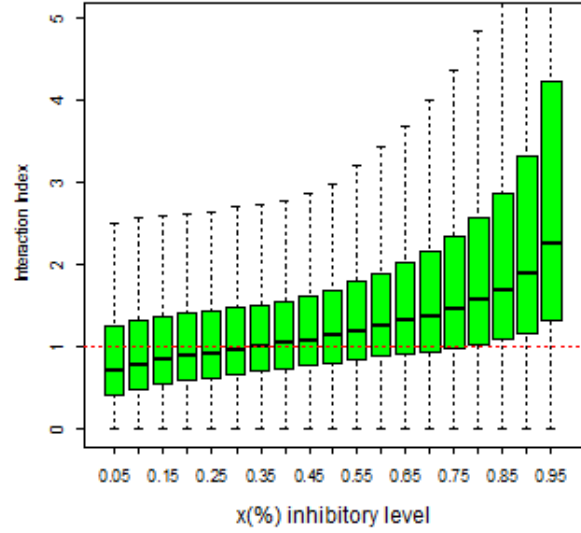
(a) DAC + SAHA



(b) DAC + TSA



(c) AZA + SAHA



(d) AZA + TSA

**Figure 3.11** Boxplots of the posterior distributions of Loewe Interaction Index versus inhibitory level in cell line SKOV3. Asterisks indicate effect levels where  $II_x$  falls below 0.95  $(1-\epsilon)$  with high probability ( $\gamma > 0.80$ ).

## Chapter 4

### Nonparametric Regression Method for Dose-Response Assessment and Drug-Drug Interaction Analysis

#### 4.1 Overview

The models described in the previous chapters make use of parametric structural models for characterizing the relationship between dose and response (e.g., Median-Effect equation,  $E_{max}$  model). In some cases, the parametric models do not fit the data. A nonparametric regression method can be useful in dealing with dose-response curves that exhibit plateaus or other local deviations from parametric models.

Splines have become a popular nonparametric (semi-parametric) tool in modeling functional data. In this chapter, we explore the use of monotone regression I-splines for dose-response assessment and drug-drug interaction analysis. This chapter can serve as a brief introduction to monotone regression I-splines and how it can be incorporated into a Bayesian hierarchical framework for dose-response assessment and drug-drug interaction analysis. The proposed Bayesian hierarchical monotone regression I-splines provide a practical and flexible nonparametric regression method for meta-analysis of independently repeated dose-response experiments. An extensive simulation study is performed to compare the nonparametric approach to the parametric approaches discussed in Chapter 2 and Chapter 3.

#### 4.2 Introduction to Montone Regression I-splines

Regression splines provide an alternative to parametric regression methods by estimating the mean curve using piece-wise functions (basis functions). The type of basis function employed (e.g., truncated polynomials, low-rank thin plate splines, natural cubic

splines, B-splines, M-splines, I-splines) may be motivated by numerical stability, ease of implementation, interpretability, or curve requirements (Ruppert, Wand, and Carroll, 2003). In the context of *in vitro* dose-response modeling, curve requirements may be smooth and monotone curves. Kelly and Rice (1990) proposed using cubic B-splines to estimate marginal dose-effect curves. Monotonicity is enforced by inequality constraints on the B-spline coefficients (e.g.,  $\beta_1 \leq \beta_2 \leq \dots \leq \beta_n$ ). B-splines have been shown to be computationally efficient; however, constraining inequalities on the coefficients can be quite cumbersome.

In this chapter, we explore the use of computationally efficient I-splines (Ramsay, 1988) for estimating the mean dose-response curve. Constraining I-spline coefficients to non-positive values (non-negative values) is sufficient to ensure non-increasing (non-decreasing) monotonicity and can be easily implemented under a Bayesian framework through prior distributions.

Consider a simple regression model

$$y_i = f(x_i) + \varepsilon_i$$

where

$$E(y|x) = f(x), \quad E(\varepsilon_i) = 0.$$

The function  $f(x)$  is a smooth curve that needs to be estimated from the  $(x_i, y_i)$ . The function  $f(x)$  can be estimated by a linear combination of  $N$  I-spline basis functions of degree  $r$ .

$$f(x_i) = \sum_{n=1}^N \beta_n I_n^r(x_i) \tag{4.1}$$

The I-spline basis functions,  $I_n^r(x)$ , are defined through their associated M-splines bases  $M_n^r(x)$ , given by a recursion formula.

$$I_n^r(x|S) = \int_L^x M_n^r(u|S) du$$

$$M_n^r(x|S) = \frac{r[(x - S_n)M_n^{r-1}(x|S) + (S_n - x)M_{n+1}^{r-1}(x|S)]}{(r-1)(S_{n+r} - S_n)}$$

$$M_n^1(x|S) = \frac{1}{(S_{n+1} - S_n)}, \quad S_n \leq x \leq S_{n+1}, \quad \text{and 0 otherwise} \quad (4.2)$$

$M_n^T(x)$  has the properties of a probability density function over the interval  $[S_n, S_{n+r}]$  where  $S=(S_1, S_2, \dots, S_{N+r})$  is a knot sequence that partitions the range of  $x$  over which  $f(x)$  is defined. In the defined interval  $[L, U]$ , the knot sequence is constructed with the following properties:

1.  $S_1 \leq \dots \leq S_{N+r}$
2.  $S_1 = \dots = S_r = L$  and  $S_{N+1} = \dots = S_{N+r} = U$
3.  $N = r + T$  where  $T$  is the number of interior knots.

Here,  $r$  and  $T$  are to be selected as well as the locations of the interior knots. Different techniques have been proposed for degree and knot location selection (Ramsay, 1998; Kelly and Rice, 1990; Wood, 1994; Rice and Wu, 2001; Di Mateo, Genovese, Kass, 2001); however, finding an optimal technique may be dependent on characteristics of the data. Figure 4.1 displays an I-spline family of degree three associated with eight interior knots.

### 4.3 Bayesian Hierarchical Monotone Regression I-splines / Bayesian Effect Interaction Index Method

#### 4.3.1 The Model

The proposed model can be used for a positive continuous response of a single agent or a combination of two agents combined at a fixed dose ratio. Let  $y_{ijk}$  be the logged measured response for experiment  $i$  replicate  $j$  at the  $k^{\text{th}}$  concentration level  $c_k$ . The data model is

$$y_{ijk} \equiv y_{ij}(c_k) = f_i(c_k) + \varepsilon_{ijk}$$

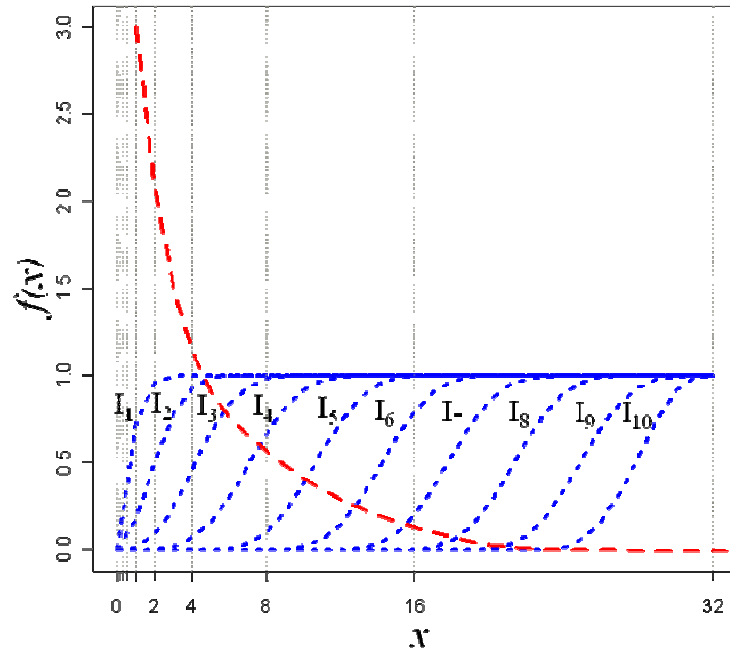


**Figure 4.1 I-spline family of degree  $r = 2$  associated with  $T = 8$  interior knots.** Note the red curve  $f(x) = \sum_{n=1}^N \beta_n I_n^r(x)$  is a linear combination of  $r + T = N = 10$  I-spline basis functions.

with  $\varepsilon_{ijk} \sim N(0, \sigma^2)$ . Here  $f_i(c_k)$  are experiment specific dose-response curves that need to be both smooth and monotone non-increasing. One way to achieve this is via I-splines (Ramsay, 1988). A linear combination of I-spline basis functions to estimate the mean response function is

$$f_i(c_k) = \alpha_i + \sum_{n=1}^{K+r-2=N} \beta_{n,i} I_n^r(c_k).$$

We include an intercept parameter  $\alpha_i$  to represent the control response, i.e., response in the absence of drug. The sum in the second term is a linear combination of  $N = K + r - 2$ , I-spline basis functions. This is a family of I-splines of degree  $r$  associated with a knot at each of  $K$  concentration levels. We use I-splines of degree three (i.e., integrated cubic M-splines) for the flexibility needed for a nonlinear curve. In an independent study, we studied the effect of using a knot at each concentration level, the effect of using fewer knots than concentration levels ( $T < K - 2$ ), and using sample quantiles of concentration to position the knots. We found if one uses too few interior knots (e.g., a single interior knot at the median or two interior knots at the terciles), local trends may not be captured and estimates may be biased. When varying the number of interior knots in a real data set application, we found the best model to be a model with a knot at each dose level; deviance information criterion (DIC) (Spiegelhalter, 2002) was used to make this assessment. A knot at each concentration level provides the flexibility desired in curve fitting. Decreasing the number of interior knots by one or two knots is unlikely to have a noticeable effect.

Since the number of concentration levels is typically small (less than 10), smoothness can be controlled through a monotonicity constraint. Under the assumption of a non-increasing monotone dose-response relationship, I-spline coefficients are constrained to non-positive values. We set the following priors for the parameters  $\alpha_i$  and  $\beta_{n,i}$ .

Priors:

$$\alpha_i \sim N(\alpha_0, \sigma_\alpha^2)$$

$$\beta_{n,i} \sim N(\beta_{0n}, \sigma_{\beta_n}^2), \quad \text{where } \beta_{n,i} \leq 0 \text{ for } n = 1, \dots, N$$

Our model assumes each experiment arises from a population of experiments. The hyper-parameters  $\alpha_0$  and  $\beta_{0n}$  represent parameters from the population level dose-response curve.

$$\mu(c_k) = \alpha_0 + \sum_{n=1}^N \beta_{0n} I_n^r(c_k)$$

Population-level curves are also enforced to be both smooth and monotone non-increasing. We set the following hyper-priors for the hyper-parameters  $\alpha_0$  and  $\beta_{0n}$ .

Hyper-priors:

$$\alpha_0 \sim N(0, 1000)$$

$$\beta_{0n} \sim N(0, 1000), \quad \text{where } \beta_{0n} \leq 0 \text{ for } n = 1, \dots, N$$

A vague Normal distribution arbitrarily centered around 0 is used for  $\alpha_0$ , and vague truncated Normal distributions are used for  $\beta_0$ 's. We use Inverse Gamma distributions on all variance parameters.

$$1/\sigma^2 \sim \text{Gamma}(0.01, 0.01)$$

$$1/\sigma_\alpha^2 \sim \text{Gamma}(0.001, 0.001)$$

$$1/\sigma_{\beta_n}^2 \sim \text{Gamma}(0.001, 0.001)$$



### 4.3.2 Bayesian Posterior Inference

One may use Markov Chain Monte Carlo (MCMC) via WinBUGS (Spiegelhalter, 2002) to simulate samples from posterior distributions of relevant parameters. Interest lies in making population (group) level inference.

#### 4.3.2.1 Dose-Response Assessment

In dose-response assessment, a quantity of interest is the inhibitory concentration ( $IC_x$  = the concentration producing  $x$  % inhibition). Posterior estimates of  $IC_x$  require a function of the parameters from the fitted model. For example, the  $g^{th}$  posterior sample of  $IC_x$  at the population level is constructed by finding the root of the following inverse function:

$$x - 1 + \exp \left\{ \sum_{n=1}^N \beta_{0n}^{(g)} I_n^r(IC_x^{(g)}) \right\} = 0 \quad (4.3)$$

The superscript ( $g = 1, \dots, G$ ) refers to saved MCMC samples used for posterior inference. The Bayesian framework provides a straightforward method for propagation of uncertainty, that is, the uncertainty in  $\beta_{0n}$ 's will propagate into uncertainty about  $IC_x$ . Informative summary statistics of  $IC_x$  can include the median and the Bayesian 95% credible interval. The Bayesian 95% credible interval is constructed with the 2.5 percentile and the 97.5 percentile and can be interpreted as an interval within which the parameter  $IC_x$  lies with probability 0.95.

A population mean dose-response curve can be displayed graphically by exponentiating posterior estimates of  $\mu(c)^{(g)} = \alpha_0^{(g)} + \sum_{n=1}^N \beta_{0n}^{(g)} I_n^r(c)$  on a grid  $[0, c_K]$ . A median-fitted response is recommended on the original scale because of skewness.

#### 4.3.2.2 Drug-Drug Interaction Analysis

We use the Bayesian Effect Interaction Index method (Hennessey et al., 2010) to assess drug-drug interaction between two agents combined at a fixed dose-ratio. The Bayesian Effect

Interaction Index method performs decision making based on the posterior distribution of Loewe Interaction Index. Posterior samples of Loewe interaction index at inhibitory level  $x$  % ( $II_x$ ) are constructed by the following function, also known as the isobole equation

$$II_x^{(g)} = \frac{IC_{x,A+B}^{(g)}}{IC_{x,A}^{(g)}} + \frac{\rho * IC_{x,A+B}^{(g)}}{IC_{x,A}^{(g)}} \quad (4.4)$$

In the numerators,  $IC_{x,A+B}$  represents the concentration of agent A in the combination (agent A + agent B) yielding  $x$  % inhibition;  $\rho = \text{dose}_B/\text{dose}_A$  is the fixed dose ratio used in the combination study. In the denominators,  $IC_{x,A}$  and  $IC_{x,B}$  represent the inhibitory concentrations of agent A alone and agent B alone, respectively, that yield the same  $x$  % inhibition. Here, the input parameters are considered random and posterior estimates are generated using the method described in Section 4.3.2.1.

The Bayesian Effect Interaction Index method performs decision making based on the posterior distribution of  $II_x$ . The decision rule is to conclude synergy (antagonism) if  $II_x$  falls below (lies above) one with high probability. Additivity is concluded in the absence of synergy or antagonism. The posterior probability that  $II_x$  falls below 1 is calculated by

$$\gamma = \Pr(II_x < 1 - \epsilon | \text{data}) \cong \frac{1}{G} \sum_{g=1}^G \mathbf{I}[II_x^{(g)} < 1 - \epsilon], \quad (4.5)$$

where  $\mathbf{I}[\cdot]$  is an indicator function. We use  $1 - \epsilon$ , for some small positive  $\epsilon$  (e.g., 0.05), rather than 1, to differentiate synergy from additivity in case  $II_x$  is close to 1. We conclude synergy if  $\gamma$  exceeds some threshold. For example, we declare "Synergy" if  $\gamma > 0.80$ . The threshold 0.80 is chosen based on prior work (Hennessey et al., 2010) that showed a threshold of 0.80 had good operating characteristics. Other threshold values that may be considered are 0.90 or 0.70. The

threshold used may be context specific, but ultimately one would want a threshold that minimizes error and maximizes correct decision making.

If interest is in additive agents and synergy is not present, the posterior probability that  $II_x$  lies above 1 is calculated.

$$\lambda = \Pr(II_x > 1 + \epsilon | data) \cong \frac{1}{G} \sum_{g=1}^G \mathbf{I} \left[ II_x^{(g)} > 1 + \epsilon \right] \quad (4.6)$$

We declare "Antagonism" if  $\lambda > 0.80$  else "Additivity" is declared.

#### 4.4 Simulation Study

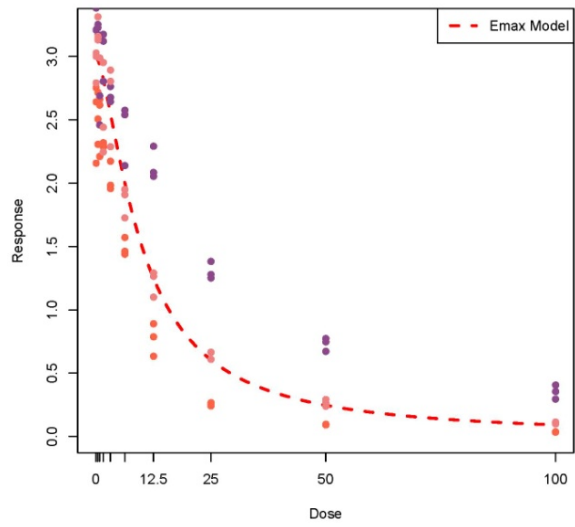
We conducted a simulation study to evaluate the performance of our proposed Bayesian Hierarchical Monotone Regression I-splines in estimating population-level dose-response curves. Performance was compared to parametric methods such as the Median-Effect Principle (Chou and Talalay, 1984) and to the Bayesian hierarchical nonlinear  $E_{max}$  model (Hennessey et al., 2010).

We performed simulations for two scenarios: (1) dose-response follows an  $E_{max}$  model and (2) dose-response deviates from an  $E_{max}$  model. For each scenario, we generated dose-response data where each realization include three independent experiments and ten concentration levels (with serial 2-fold changes). Each experiment included three replicates per dose level yielding 30 observations per experiment and 90 observations per realization. We included the following variation in the generated data: variation within-experiment (between-replicates), variation between-experiments, variation in the responses of the controls, and heteroscedasticity. All variations were set to values similar to those observed in the real data.

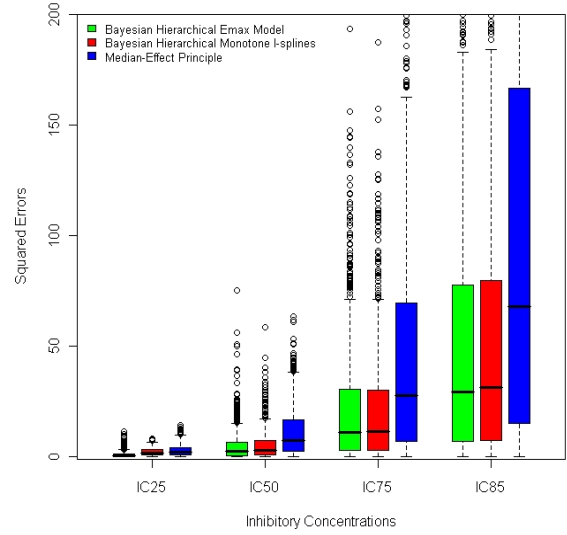
For Scenario 1, we generated dose-response data for two hypothetical agents, agent A and agent B, for which the true dose-response relationship is characterized by an  $E_{max}$  model. We generated dose-response data for agent A for which the true response curve is  $Y =$

$3/[1+(C/10)^{3/2}]$ . This is an Emax model with parameter values  $E_0 = 3$ ,  $IC_{50} = 10$ , and  $M = 3/2$ . With the idea that experiment-specific curves deviate from the true population mean curve and replicates within experiment deviate from their experiment specific mean curve, we proceeded with the following: sample experiment specific  $E_{0,i}$  from a log-normal distribution to constrain values to be positive; sample  $IC_{50,i}$  and  $M_i$  from a bivariate log-normal distribution to constrain positive values and to introduce plausible correlation between the two parameters; use a multiplicative error term to ensure positive data points and introduce heteroscedasticity; set the within-experiment variation to  $\sigma^2 = 0.01$ ; set the between-experiment parameter variation for  $IC_{50}$  to  $\sigma_{IC_{50}}^2 = 16$ ; and allow for minimal variation between-experiments in the controls and the shapes of the curves represented by  $\sigma_{E_0}^2 = 0.02$  and  $\sigma_M^2 = 0.018$ . The same was done for agent B with the exception that we used different parameter values and smaller between-experiments variation represented by  $\sigma_{IC_{50}}^2 = 0.30$ .

Figures 4.2(a) and 4.3(a) display the true curves for hypothetical agent A (Fig. 4.2a) and agent B (Fig. 4.2b) for one sample realization of simulated data. Figure 4.2(b) and 4.3(b) are the distributions of the squared errors in estimating  $IC_{25}$ ,  $IC_{50}$ ,  $IC_{75}$ , and  $IC_{85}$  with fitted Bayesian Hierarchical Emax model (green boxplot), Bayesian Hierarchical Monotone I-splines (red boxplot), and Median-Effect Principle (blue boxplot). From the boxplots of the squared errors, we conclude that the Bayesian Hierarchical Emax model performs the best under Scenario 1; however, not much is lost by using the nonparametric Bayesian Hierarchical Monotone I-splines model. We find that performance decreases with increasing inhibitory levels, but the Median-Effect Principle's precision tends to decrease at a higher rate compared to the Bayesian Hierarchical Emax model and the Bayesian Hierarchical Monotone I-splines. The same trend is observed for hypothetical agent B, but at a smaller magnitude associated with smaller between-experiment variations.



(a)



(b)

**Figure 4.2 Simulation results for Scenario 1 hypothetical agent A.** (a) The simulation truth is that response follows an Emax model  $Y = 3 / [1 + (C/10)^{3/2}]$ . The red dashed curve represents the simulation truth for hypothetical agent A, and the points represent one realization from the simulated data. (b) The distribution of the squared errors in estimating inhibitory concentrations with fitted Bayesian Hierarchical Emax model (green boxplot), Bayesian Hierarchical Monotone I-splines (red boxplot), and the Median-Effect Principle (blue boxplot).

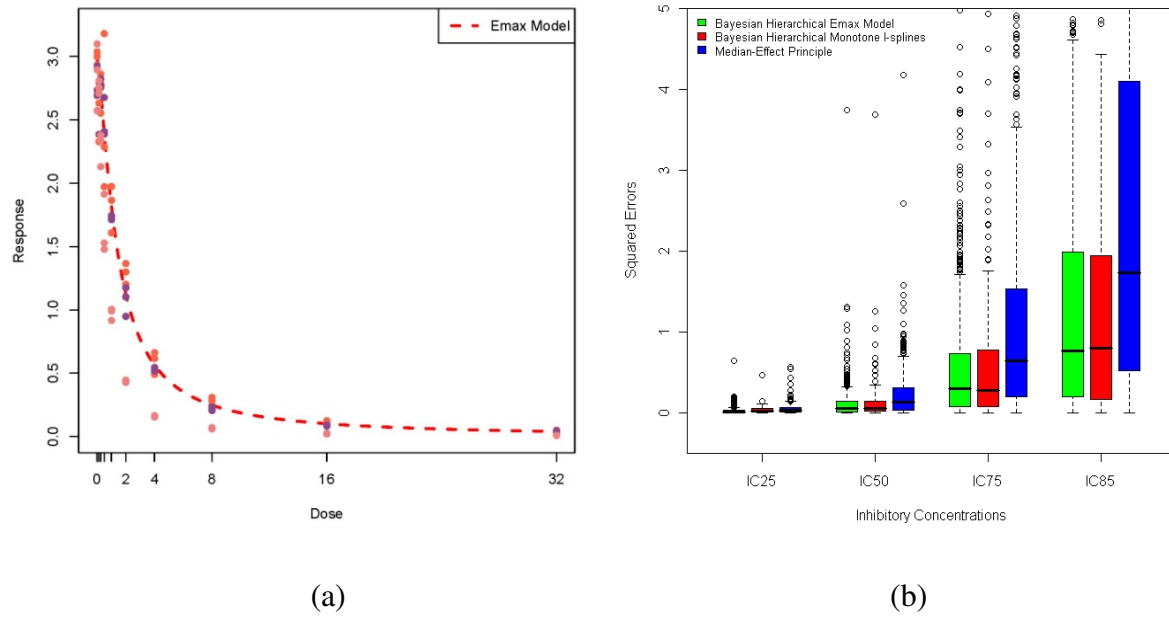


**Figure 4.3 Simulation results for Scenario 1 hypothetical agent B.** (a) The simulation truth is that response follows an Emax model  $Y = 3 / [1+(C/1.38)^{1.37}]$ . The red dashed curve represents the simulation truth for hypothetical agent B, and the points represent one realization from the simulated data. (b) The distribution of the squared errors in estimating inhibitory concentrations with fitted Bayesian Hierarchical Emax model (green boxplot), Bayesian Hierarchical Monotone I-splines (red boxplot), and the Median-Effect Principle (blue boxplot).

In Scenario II, we generated dose-response data for which the true response deviates from an  $E_{max}$  model. Specifically, we generated dose-response data for agent C, such that the true response curve is a weighted sum of two  $E_{max}$  models (double sigmoid model)  $Y = 0.90 * 3 / [1 + (C/10)^{3/2}] + 0.10 * 3 / [1 + (C/50)^{3/20}]$ , and for agent D, such that the true response curve is an asymmetric sigmoid model (Richard's function)  $Y = 3 / [1 + (C/5)^{1.37}]^{1/2}$ . Figures 4.4(a) and 4.5(a) display the true curves for hypothetical agent C (Fig. 4.4a) and agent D (Fig. 4.5a), respectively, for one realization of the simulated data. The double-sigmoid model provides a slight deviation from the Emax model  $Y = 3 / [1 + (C/10)^{3/2}]$ . The asymmetric sigmoid model provides a large deviation from the Emax model  $Y = 3 / [1 + (C/5)^{1.37}]$ . From Figure 4.4b and Figure 4.5b we conclude that the Bayesian Hierarchical Monotone I-splines provides a gain in performance over parametric methods when there is a deviation from a parametric  $E_{max}$  model.

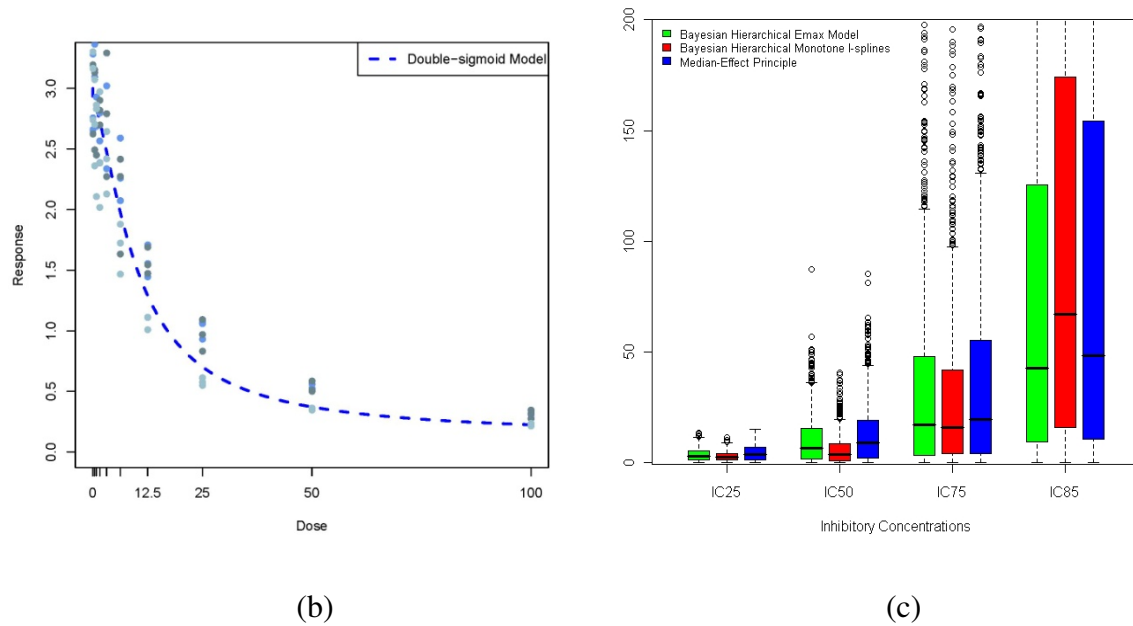
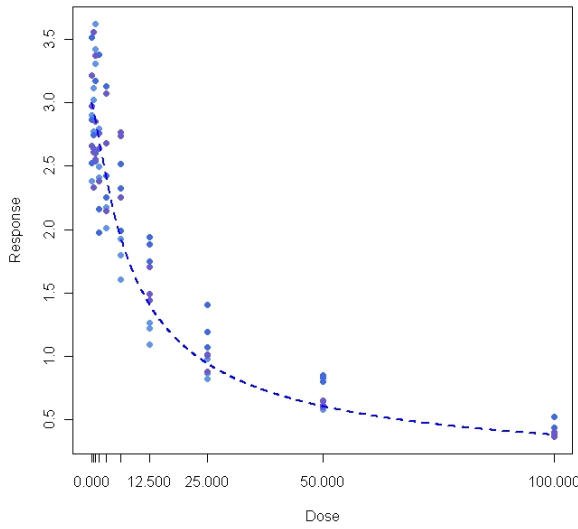
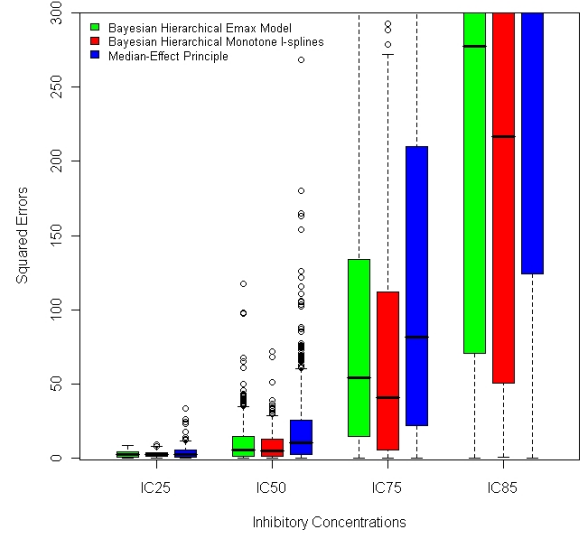


**Figure 4.4 Simulation data for Scenario 2 hypothetical agent C.** (a) Simulation truth for agent C under Scenario 2 where response deviates from an Emax model. The blue dashed curve represents the simulation truth for hypothetical agent C where response follows a weighted sum of two Emax models (double-sigmoid model)  $Y = 0.90 \cdot 3 / [1 + (C/10)^{-3/2}] + 0.10 \cdot 3 / [1 + (C/50)^{-3/20}]$ . The points represent one realization from the simulated data. (b) The distribution of the squared errors in estimating inhibitory concentrations with fitted Bayesian Hierarchical Emax model (green boxplot), Bayesian Hierarchical Monotone I-splines (red boxplot) and the Median-Effect Principle (blue boxplot).





(b)



(c)

**Figure 4.5 Simulation data for Scenario 2 hypothetical agent D.** (a) Simulation truth for agent C under Scenario 2 where response deviates from an Emax model. The blue dashed curve represents the simulation truth for hypothetical agent C where response follows a Richards function  $Y = 3 / [1 + (C/5)^{1.37}]^{1/2}$ . The points represent one realization from the simulated data. (b) The distribution of the squared errors in estimating inhibitory concentrations with fitted Bayesian Hierarchical Emax model (green boxplot), Bayesian Hierarchical Monotone I-splines (red boxplot) and the Median-Effect Principle (blue boxplot).

## Chapter 5

### Concluding Remarks

The work presented in this dissertation makes an original contribution to the fields of biostatistics, drug discovery, and toxicology. The main contributions of this dissertation are (1) parametric and nonparametric regression methods that make sound predictions of *in vitro* dose-response relationships, (2) a more precise method to estimate inhibitory concentrations, and (3) a novel method that improves the screening process of effective/synergistic agents and reduces the incidence of reaching false positive conclusions.

It is important to assess *in vitro* dose response and drug interaction correctly. This is because there is a potential risk of toxicity in humans and animals when drugs are administered. It is shown that the conventional method, the Median-Effect Principle/ Combination Index Method, leads to inefficiency by ignoring important sources of variation inherent in dose-response data and discarding data points that do not agree with the Median-Effect Principle. Rouder and Lu (2005) suggest that unmodeled variability can lead to problematic inference. This is in agreement with our simulation study that showed analyses with the Median-Effect Principle/Combination Index Method yield a high incidence of type I error and in some cases, low power to detect synergy. This can result in resources being allocated to agents with undesirable interaction and promising agents being over looked.

In Chapter 3 we proposed a novel methodology for dose-response assessment and drug-drug interaction analysis. The proposed Bayesian Hierarchical Nonlinear  $E_{max}$  model / Bayesian Effect Interaction Index method accounts for various sources of variation and uncertainty, enabling a more efficient and reliable inference. The proposed Bayesian Hierarchical Nonlinear  $E_{max}$  model consists of a modified Hill's model ( $E_{max}$  model) with an additive residual error on

the logarithmic scale. Both the  $E_{max}$  model and the Median-Effect equation conform to the mass action law principle. The Median-effect equation is a simpler form for relating dose and response; however, ignoring the variation in the control response could render problematic inference on the median inhibitory concentration,  $IC_{50}$ . We use an  $E_{max}$  model instead of the Median-Effect equation (2.1), because the Median-Effect equation assumes that the control response is fixed and equal to one. The  $E_{max}$  model does not assume the control response is equal to one and allows one to model the variation in the controls through the parameter  $E_0$ .

Simulation studies show that the Bayesian Hierarchical Nonlinear  $E_{max}$  model provides a more reliable estimator of the population-level dose-response curve; the Bayesian hierarchical nonlinear  $E_{max}$  model provides a more precise estimator for  $IC_{25}$ ,  $IC_{50}$ ,  $IC_{75}$ , and  $IC_{85}$  compared to meta-analysis with the Median-Effect Principle. We find performance depends on the magnitude of variation between experiments, the level of inhibition, and if the parameter estimate lies in a flat region of the dose-response curve or requires extrapolation beyond the investigating dose levels. For the Bayesian Hierarchical Nonlinear  $E_{max}$  model, we find that increasing the sample size from three to six experiments reduces the median squared error as much as 50%. This was not observed with meta-analysis Median-Effect Principle. Performance with the Median-Effect Principle did not improve with increasing sample size, suggesting that meta-analysis with the Median-Effect Principle does not provide a consistent estimator.

The proposed Bayesian Hierarchical Nonlinear  $E_{max}$  model method also allows for *a priori* knowledge to be incorporated into the current analysis. We address *a priori* knowledge, because information about a single-agent's median inhibitory concentration can often be extracted from previous studies or literature. We did not jointly model the single-agents and the combination, however, this can be done to borrow strength across agents.

In Chapter 3 we also introduced the Bayesian Effect Interaction method. The Bayesian Effect Interaction method allows one to quantitatively assess interaction between two agents combined at a fixed dose ratio. The proposed method bases decision making on the posterior distribution of Loewe interaction index and makes a comprehensive and honest accounting of uncertainty. The Bayesian Effect Interaction Index method with threshold  $\gamma > 0.80$  and  $\gamma > 0.90$  displayed good operating characteristics under an additive drug combination scenario (sham experiment). This was not observed for the Median-Effect Principle, which yielded a high incidence of type I error, that is, rejecting additivity when, in fact, additivity is true. Additivity agents may be meaningful to drug developers interested in no interaction.

The Bayesian Effect Interaction Index method with threshold  $\gamma > 0.70$  and  $\gamma > 0.80$  displayed good operating characteristics under a strong synergistic interaction scenario. The more problematic scenario was when the interaction was quantitatively changing, that is, the values of the interaction index changed significantly over a narrow range of inhibitory levels. Most of the time, the Bayesian Effect Interaction Index method was able to declare synergy correctly, but performance declined as the interaction qualitatively changed from synergy to additivity to antagonism. Increasing the sample size (number of experiments) from three to six improved the interaction analysis over a larger range of inhibitory levels. We recommend increasing the number of experiments if it would improve prediction from *in vivo* or clinical studies.

Boik et al. (2008) proposed a related nonlinear mixed-effects model. Their model differs from ours in several ways. They consider a single experiment with replicate multi-well trays performed simultaneously. A random tray effect is only considered on the control response parameter  $E_0$ ;  $IC_{50}$  and  $M$  are considered fixed effects. Our model considers independently repeated experiments that are subject to between-experiment variation. We

model the between-experiment variation by allowing the parameters  $E_0$ ,  $IC_{50}$ , and  $M$  to vary across experiments. For drug interaction analysis, Boik et al. (2008) proposed the MixLow method. The MixLow is also based on Loewe additivity, but relies on asymptotics for inference. Asymptotics rely on large sample theory and may not be appropriate in a small sample (number of experiments) setting. Our proposed method does not rely on asymptotics and may be more appropriate.

The aforementioned methods make use of a parametric structural model (e.g., Median-Effect equation,  $E_{max}$  model) to characterize the relationship between response and dose. In some cases the parametric models do not fit the data. In Chapter 4, we provided an alternative non-parametric regression method. The proposed Bayesian Hierarchical Monotone Regression I-splines can be useful in dealing with dose-response curves that exhibit plateaus or other local deviations from parametric models.

## Appendix A

### WinBUGS Code for Bayesian Hierarchical Nonlinear $E_{max}$ model

In the data list, one would include the vector of measured responses (Y), the vector of unique concentration levels (conc), a pointer for looping over replicates (offset), the number of experiments (I), and the number of concentration levels (K).

```
model{
  for(i in 1:I){ # loop over experiments
    for(k in 1:K){ # loop over concentration
      for(l in offset[(i-1)*K+k]:(offset[(i-1)*K+k+1]-1)){#replica
        Y[l]~dlnorm(mu.lognormal[i,k], tau.lognormal)
      }
      mu.lognormal[j,k]<-log(mu[j,k])-(1/(2*tau.lognormal))
      mu[i,k]<-exp(logEmaxHEY[i])/(1+ pow((conc[k]/
        exp(logIC50[i])),exp(logm[i])))
    }
    logEmaxHEY[i]~dnorm(theta.logEmax[i],tau.logEmax)
    logIC50[i]~dnorm(theta.logIC50[i],tau.logIC50)
    logm[i]~dnorm(theta.logm[i],tau.logm)

    theta.logEmax[i] <- mu.logEmax + xi.logEmax*eta.logEmax[i]
    theta.logIC50[i] <- mu.logIC50 + xi.logIC50*eta.logIC50[i]
    theta.logm[i] <- mu.logm + xi.logm*eta.logm[i]
  }
  tau.lognormal~dgamma(0.01,0.01)
```

```

mu.logEmax~dnorm(0, 0.001)
mu.logIC50~dnorm(0, 0.001)
mu.logm~dnorm(0, 0.001)

xi.logEmax~dnorm(0, tau.xi.logEmax)
xi.logIC50~dnorm(0, tau.xi.logIC50)
xi.logm~dnorm(0, tau.xi.logm)

tau.xi.logEmax <- pow(prior.scale.logEmax, -2)
tau.xi.logIC50 <- pow(prior.scale.logIC50, -2)
tau.xi.logm <- pow(prior.scale.logm, -2)

for(e in 1:I){
  eta.logEmax[e]~dnorm(0, tau.eta.logEmax)
  eta.logIC50[e]~dnorm(0, tau.eta.logIC50)
  eta.logm[e]~dnorm(0, tau.eta.logm)
}

tau.eta.logEmax~dgamma(.5, .5)
tau.eta.logIC50~dgamma(.5, .5)
tau.eta.logm~dgamma(.5, .5)

sigma.logEmax <- abs(xi.logEmax)/sqrt(tau.eta.logEmax)
sigma.logIC50 <- abs(xi.logIC50)/sqrt(tau.eta.logIC50)
sigma.logm <- abs(xi.logm)/sqrt(tau.eta.logm)

```

```
tau.logEmax <- 1/(sigma.logEmax*sigma.logEmax)
tau.logIC50 <- 1/(sigma.logIC50*sigma.logIC50)
tau.logm <- 1/(sigma.logm*sigma.logm)
}
```



## Appendix B

### WinBUGS Code for Bayesian Hierarchical Monotone Regression I-splines

In the data list, one would include the vector of log (base  $e$ ) transformed measured responses ( $\log Y$ ), the design matrix for the I-splines ( $I$ ), the number of basis used to estimate mean function ( $N_{\text{basis}}$ ), a pointer for looping over replicates ( $\text{offset}$ ), the number of experiments ( $E$ ), and the number of concentration levels ( $K$ ).

```
model{

  for(e in 1:E){ # Loop over Experiments

    for(k in 1:K){ # Loop over Concentration

      for(l in offset[(j-1)*10 + k]:(offset[(j-1)*10 + k + 1]-1)){

        logY[l]~dnorm(mu[j,k],tau.y)

      }

      mu[j,k]<- alpha[j]- beta[j,1]*I[k,1] - beta[j,2]*I[k,2] -

        ...- beta[j,N]*I[k,Nbasis]

    }

  }

  for(experiment in 1:E){

    alpha[experiment]~dnorm(alpha0,tau.alpha)

  }
```

```

for(experiment in 1:E){

  for(N in 1:Nbasis){

    beta[experiment,N]~djl.dnorm.trunc(beta0[N], tau.beta[N],

                                         0.0, 1.0E-6)

  }

}

alpha0~dnorm(1.0,1.0E-3)

for(N in 1:Nbasis){

  beta0[N]~djl.dnorm.trunc(0.0,1.0E-3,0.0,1.0E-6)

}

tau.y~dgamma(1.0E-3,1.0E-3)

tau.alpha~dgamma(1.0E-3,1.0E-3)

for(N in 1:Nbasis){

  tau.beta[N]~dgamma(1.0E-3,1.0E-3)

}

}

```

## Bibliography

1. Berenbaum, M. C. (1989). What is synergy? *Pharmacological Reviews* **41**, 93–141.
2. Bickel, P. J., and Doksum, K. A. (2001). *Mathematical Statistics: Basic Ideas and Selected Topics*. New Jersey:Prentice Hall, pp. 306-314.
3. Bliss, C. I. (1939). The toxicity of poisons applied jointly. *Annals of Applied Biology* **26**:585-615.
4. Boik, J. C., Newman, R. A., and Boik, R. J. (2008). Quantifying synergism/antagonism using nonlinear mixed-effects modeling: A simulation study. *Statistics in Medicine* **27**, 1040–1061.
5. Chou, T. C. (1976). Derivation and properties of Michaelis-Menten type and Hill type equations for reference ligands. *Journal of Theoretical Biology* **59**, 253–276.
6. Chou, T. C. (2006). Theoretical basis, experimental design, and computerized simulation of synergism and antagonism in drug combination studies. *Pharmacological Reviews* **58**, 621–681.
7. Chou, T. C. and Rideout, D. D. (1991). *Synergism and Antagonism in Chemotherapy*. San Diego: Academic Press.
8. Chou, T. C. and Talalay, P. (1984). Quantitative analysis of dose-effect relationships: The combined effects of multiple drugs or enzyme inhibitors. *Advances in enzyme regulation* **22**, 27–55.
9. Crainiceanu, C.M., Ruppert, D., Wand, M.P. (2005). Bayesian Analysis for Penalized Spline Regression Using WinBUGS. *Journal of Statistical Software* **14**:11.
10. Davidian, M., Giltinan, D.M. (1995). *Nonlinear models for repeated measurement data*. New York: Chapman and Hall.

11. DiMatteo, I., Genovese, C.R., Kass, R.E. (2001). Bayesian Curve-Fitting with Free-Knot Splines. *Biometrika*, **88**:4, 1055-1071.
12. Dunson, D. B. (2001). Commentary: Practical advantages of Bayesian analysis of epidemiologic data. *American Journal of Epidemiology* **153**, 1222–1226.
13. Gelman, A. (2006). Prior distributions for variance parameters in hierarchical models. *Bayesian Analysis* **1**, 515–533.
14. Gelman, A. and Hill, J. (2007). *Data Analysis Using Regression and Multilevel/Hierarchical Models*. New York: Cambridge University Press.
15. Gelman, A., Carlin, J. B., and Rubin, D. B. (2004). *Bayesian Data Analysis*, 2nd edition. London: Chapman and Hall.
16. Goldoni, M. and Johansson, C. (2007). A mathematical approach to study combined effects of toxicants in vitro: Evaluation of the Bliss independence criterion and the Loewe additivity model. *Toxicology In Vitro Cancer Research* **5**, 759–769.
17. Greco, W. R., Park, H. S., and Rustum, Y. M. (1990). Application of a new approach for the quantitation of drug synergism to the combination of cis-diamminedichloroplatinum and 1- $\beta$ -Darabinofuranosylcytosine. *Cancer Research* **50**, 5318–5327.
18. Greco, W. R., Bravo, G., and Parsons J. C. (1995). The search for synergy: A critical review from a response surface perspective. *Pharmacological Reviews* **47**, 331–385.
19. Hennessey, V. G., Rosner, G. L., Bast Jr., R. C., Chen, M. (2010). A Bayesian Approach to Dose-Response Assessment and Synergy and Its Application to In Vitro Dose-Response Studies. *Biometrics*.
20. Hill, A. V. (1910). The possible effects of the aggregation of the molecules of haemoglobin on its dissociation curves. *The Journal of Physiology* **40**, iv–vii.

21. Kelly, C., and Rice, J. (1990). Monotone Smoothing with Application to Dose-Response Curves and the Assessment of Synergism. *Biometrics* **46**, 1071-1085.
22. Lee, J. J. and Kong M. (2007). Confidence intervals of interaction index for assessing multiple drug interaction. *Statistics in Biopharaceutical Research*. Available at: <http://www.amstat.org>.
23. Lee, J. J., Kong M., Ayers, G. D., and Lotan, R. (2006). SYNERGY. Available at: <http://biostatistics.mdanderson.org/SoftwareDownload>.
24. Lee, J. J., Kong M., Ayers, G. D., and Lotan, R. (2007). Interaction index and different methods for determining drug interaction in combination therapy. *Journal of Biopharmaceutical Statistics* **17**, 461–480.
25. Loewe, S. (1928). Die quantitation probleme der pharmakologie. *Ergebn. Physiol* **27**, 47–187.
26. Loewe, S., Muischnek, H., (1928). Effect of combinations: mathematical basis of problem. *Arch. Exp. Pathol. Pharmacol.* **114**:313–326.
27. Neelon, B., and Dunson, D.B. (2004). Bayesian Isotonic Regression and Trend Analysis. *Biometrics* **60**, 398-406.
28. Petersdorf, R. G., Page, W. F., and Thaul, S., Editors. (1996). Committee to Study the Interactions of Drugs, Biologics, and Chemicals in U.S. Military Forces. *Interactions of Drugs, Biologics, and Chemicals in U.S. Military Forces*. Washington, DC: The National Academy Press.
29. Qui, J. (2006). Epigenetics: Unfinished symphony. *Nature*. **441**, 143-145.
30. Ramsay J., (1988). Monotone regression splines in action. *Statistics in Sciences*. **3**:4, 425-441.

31. Rice, J.A., Wu, C.O. (2001). Nonparametric Mixed Effects Models for Unequally Sampled Noisy Curves. *Biometrics*, **57**:1, 253-259.
32. Rouder, J. N. and Lu, J. (2005). An introduction to Bayesian hierarchical models with an application in theory of signal detection. *Psychonomic Bulletin & Review* **12**, 573–604.
33. Ruppert, D., Wand M.P., Carroll, R.J. (2003). *Semiparametric regression*. Cambridge University Press.
34. Skehan P., Storeng R., and Scudiero D., et al. (1990). New colorimetric cytotoxicity assay for anticancer-drug screening. *Journal of the National Cancer Institute* **82**, 1107–1112.
35. Spiegelhalter, D., Thomas, A., Best, N., and Lunn, D. (2002). WinBUGS 1.4 manual. Available at: <http://www.mrc-bsu.cam.ac.uk/bugs>.
36. Spiegelhalter, David J.; Best, Nicola G.; Carlin, Bradley P.; van der Linde, Angelika (October 2002). Bayesian measures of model complexity and fit (with discussion). *Journal of the Royal Statistical Society, Series B (Statistical Methodology)* **64** (4): 583–639.
37. Tallarida, R. J. and Raffa, R. B. (1996). Testing for synergism over a range of fixed ratio drug combinations: replacing the isobologram. *Life Sciences* **58**, 23–28.
38. Wood, S.N., (1994). Monotonic Smoothing Splines Fitted by Cross Validation. *SIAM Journal on Scientific Computing* **15**:5, 1126-1133.

## Vita

September 14, 1977 ..... Born, Houston, Texas

May, 2003 ..... B.S. Computer Science  
Texas State University

August, 2005 ..... M.S. Applied Mathematics,  
University of Nevada, Las Vegas

August, 2005.....Entered the University of Texas  
Health Science Center at Houston Graduate  
School of Biomedical Sciences

### Publications/Ongoing Projects

1. Hennessey, V. G., Rosner, G. L., Bast, R. C., and Chen, M (2010). A Bayesian Approach to Dose-Response Assessment and Synergy and Its Application to In Vitro Studies. *Biometrics*, accepted for publication Jan 6, 2010.
2. Hennessey, V. G., Baladandayuthapani, V., and Rosner, G. L., Bast, R. C., and Chen, M. Bayesian Hierarchical Monotone Regression I-Splines for Dose-Response Assessment and Drug Interaction Analysis, ready to submit.
3. Hennessey, V. G., Li, J., Zhu, L., Huang, X., Chi, E., Yuan, Y. A Bayesian Hybrid Selection Model for Analysing Clinical Longitudinal Data with Competing Risks Nonignorable Dropout, in preparation.
4. Chen, M., Lu, Z., Bornmann, W. G., Hennessey, V. G. , Rosner, G. L., Yu, Y., Ahmed, A. A., Das, P., Liao, W. S., Bast Jr., R. C. Combination Effect of Demethylating Agents and Histone Deacetylase Inhibitors in Ovarian Cancer-A Novel Approach, ready to submit.